

Thermal Remagnetization in Polycrystalline Permanent Magnets

by

R. Schumann[†] and L. Jahn^{††}

[†]*Institute for Theoretical Physics, TU Dresden, D-01062 Dresden, Germany*

^{††}*Institute for Applied Physics, TU Dresden, D-01062 Dresden, Germany*

Abstract

The thermal remagnetization (TR), i.e. the reentrance of magnetization upon heating in a steady-field demagnetized sample, is a common feature to the four types of polycrystalline permanent magnets, mainly utilized for practical purposes, i.e. barium ferrites, $SmCo_5$, Sm_2Co_{17} and $NdFeB$ magnets. The effect is small for pinning controlled and large for nucleation controlled magnets. The effect is strongly dependent on the demagnetization factor and may reach nearly 100% in $SmCo_5$ samples measured in a closed circuit. The TR is very sensitive to a small superimposed steady field. The maximum effect and the position of the peak is dependent on the initial temperature. The direction of the TR is correlated with the temperature coefficient of the coercivity, resulting in a inverse TR in barium ferrite. The susceptibility of the thermally remagnetized samples is increased. Repeated cycles of steady-field demagnetization followed by heating result in the same TR. The phenomenology of TR and ITR is explained by means of a model taking into account both the internal field fluctuations due to grain interactions and the decay of single domain grains into multi-domain state. By taking the measured temperature dependencies of the coercivity and the saturation magnetization the theory is able to reproduce the experiments very well, allowing to determine the width of the field fluctuations, the width of the switching field distribution and an internal demagnetization factor as characteristics of the materials by fitting.

KEYWORDS: permanent magnets, thermal remagnetization, interaction fields, switching field distribution

PACS: 75.50Vv, 75.50Ww, 75.60Ej

CORRESPONDING AUTHOR: R. Schumann

E-MAIL: *schumann@theory.phy.tu-dresden.de*

1 Introduction

The effect of Thermal Remagnetization (TR) was first mentioned in a paper of Lifshits, Lileev and Menushenkov [1] devoted to stability investigations of the coercivity of $SmCo_5$ -magnets at elevated temperatures in 1974. They wrote: "We also found a remagnetization upon heating in absence of an external field at samples, which were partially or completely demagnetized by a steady counter field." [2]. One year later the same group [3] published a first systematic study devoted solely to this effect. As we will see in the following, TR is not restricted to $SmCo_5$ magnets, instead it is quite common to all sintered hard magnets. But, before giving an outline of the history, we have to explain the principle of the TR experiment. In Fig. 1 the experimental procedure

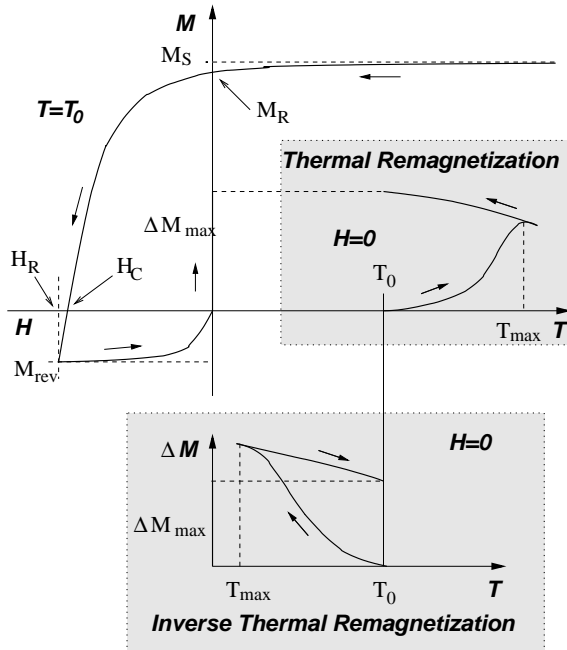


Figure 1: The scheme of the standard TR-Experiment. After saturation the sample is demagnetized isothermally by a steady field at the initial temperature T_0 (upper sketch) and afterwards either heated (TR-experiment - left shaded picture) or cooled (ITR-experiment) with the external magnetic field switched off, whereby the magnetization is measured.

is sketched. Firstly the sample has to be saturated by a very large magnetic field. Next a steady field H_R (remanence coercivity) opposite to the saturation direction is applied. Switching off the external field drives the sample in the dc-demagnetized state. Now the temperature is changed and the related change of magnetization is measured. If a reentrance of magnetism with increasing temperature is observed the effect is called thermal remagnetization (TR), see the right shaded picture. Otherwise, if a magnetization return is observed upon cooling, as shown in the lower shaded figure, we call it inverse thermal remagnetization (ITR). Already in their first investigations Lileev et al. [1, 3] demonstrated for $SmCo_5$, that the TR is strongly dependent on the demagnetization factor, especially it amounts up to nearly 100 % in a closed circuit. Furthermore it was shown, that at least for $SmCo_5$, the effect is not necessary restricted to the demagnetized state, but also occurs in a partially dc-demagnetized state (± 23 % of the saturation magnetization). On the other hand the effect is absent in ac-demagnetized samples. Reconsidering the TR in $SmCo_5$ nearly ten years later, Livingston and Martin [4] suggested as explanation of the TR the conversion of the single domain state (SDS) of some grains into a multidomain state (MDS). This assumption was supported by the observation of multidomain states in a few big grains of $SmCo_5$ at higher temperature and also by the discovery of the TR in sintered $NdFeB$ -magnets [5], where the effect is larger in samples with lower number of multidomain grains in the dc-demagnetized state. An alternate explanation was given in Ref. [6]. Based on investigations of the TR in $SmCo_5$ and barium ferrite in 1985 the authors proposed the magnetic interaction between adjacent grains together with a broad distribution of the temperature dependent switching fields to be responsible for the TR. This model, despite of its oversimplifications, was able to explain the increase of magnetization qualitatively and it showed the key role of the temperature coefficient of the coercivity resulting in the discover-

ing of the ITR for sintered barium ferrites. Furthermore it was demonstrated that the TR is connected with a increasing susceptibility and that small external fields may suppress the effect at all. Additional support the interaction model got from a paper of Lileev and Steiner [7], proving that the TR effect depends strongly on the volume packing density, a fact which was shown to be responsible for the difference in ITR in sintered and chemical precipitated barium ferrite samples [6]. To decide, which of the both models accounts well for the observed effects Lileev et al. [8, 9] counted carefully grains in single-domain state and multi-domain state at different temperatures. Their results proved that there is a delicate interplay of both interaction and formation of multi-domain grains, at least in the $SmCo_5$ samples. From the very beginning it was assumed that TR is connected with the nucleation controlled magnets. Otherwise, pinning controlled magnets should not show the effect, and indeed, the $SmCo_5$ -, $NdFeB$ -, and ferrite-magnets show remarkable TR and ITR resp. [3, 4, 5, 6, 10, 11, 12], whereas the effect in Sm_2Co_{17} is small [13]. To what extend this statement is true together with the role of interaction in relation to the decay of SDS grains into MDS grains, motivated much of the theoretical and experimental work. Since the effect is most conspicuous in $SmCo_5$, much effort was spent to this material. Otherwise it became clear, that it is a rather common effect to all modern polycrystalline permanent magnets. Nevertheless, as will be shown in the next section, the experiments demonstrate clearly the individuality of every compound class. Regarding the nucleation controlled magnets we find that both the saturation magnetization and the coercivity decrease monotonously for $SmCo_5$ - and $NdFeB$ -magnets, but, while in $NdFeB$ magnets the coercivity and the saturation magnetization vanish at nearly the same temperature, in $SmCo_5$ the coercivity reaches zero at considerable lower temperature than the saturation magnetization. In contrast barium ferrite shows an increasing coercivity up to 550 K, i.e.

Type	No. of phases	coercivity mechanism	$\frac{dH_C}{dT}$
$SmCo_5$	1	nucleation	+
Sm_2Co_{17}	cellular	pinning	+
$NdFeB$	≥ 2	nucleation	+
Ba-Ferrite	1	nucleation	-

Table 1: Some of the main characteristics of the four groups of sintered permanent magnets.

the temperature coefficient of the coercivity has the opposite sign. For the Sm_2Co_{17} -magnets $M_S(T)$ and $H_C(T)$ behave as in $SmCo_5$, but there we have a complete different coercivity mechanism, i.e. volume pinning of domain walls. In $NdFeB$ magnets the magnetic active phase is separated by one or more other phases reducing the interaction between adjacent grains. In Tab. 1 we show schematically how the four groups of magnetic materials are qualitatively distinguished by some features being relevant for TR, i.e. the number of phases, the coercivity mechanism, and the temperature coefficient of the coercivity.

In the third chapter, we will give a brief review over the models used so far to understand the different aspects of TR and present a theory which accounts for both the TR in $SmCo_5$ and the ITR in barium ferrite in single-phase magnets. The last chapter will be summarize what can be learned from TR measurements and some remarks to open questions will be appropriate.

2 Experiments

2.1 The standard TR experiment in the $SmCo_5$, Sm_2Co_{17} and $NdFeB$

Sintered $SmCo_5$ -magnets for which TR experiments are reported are single-phased and exhibit a poly-crystalline structure with the typical grain sizes much bigger than the critical radius for single domain behavior. They are mainly well textured. The phase diagram [14, 15] of the Sm-Co system shows

that below about 750 °C the magnetic active phase $SmCo_5$ is meta-stable with respect to a decomposition into Sm_2Co_7 and Sm_2Co_{17} with reduced uniaxial anisotropy. While at moderate temperatures this decomposition process does not affect the microstructure and the magnetic quantities, chemical instability becomes a problem in high temperature measurements, since a long lasting TR experiment may act as an unintentional heat treatment of a sample. The first measurements of the TR in $SmCo_5$ are collected in Fig. 2. The points shown as squares are taken from Ref. [3] and the triangles from Ref. [4] and the open circles are our own measurements at a VACOMAX 200 specimen [16]. The biggest TR (filled squares) was measured in a closed magnetic circuit what corresponds to zero demagnetization factor. The remaining curves represent open circuit measurements at cylindrical samples of different aspect ratio resulting in different demagnetization factors. In Ref. [3] the remanence was measured at room temperature after heating to a certain temperature and cooling down to room temperature, whereas in Ref. [4] the magnetization was registered simultaneously while increasing the temperature stepwise. Every temperature step was followed by an annealing of 30 min. The remaining curves were measured while continuously increasing the temperature. In order to get the slightly differing experiments into one diagram we used the temperature dependence of M_S measured at our VACOMAX 200 sample together with the room temperature remanence data given in Refs. [3, 4] to scale the results. Although one may object that the results of Fig. 2 stem from $SmCo_5$ samples produced in different ways, it is evident that a variation of the demagnetization factor influences the TR much stronger than a variation of the production conditions, at least if the result is a good $SmCo_5$ hard magnet. Fig. 3 shows both the TR for two samples with different demagnetization factors cut from the same material (VACOMAX 170) [16], and the temperature dependence of the

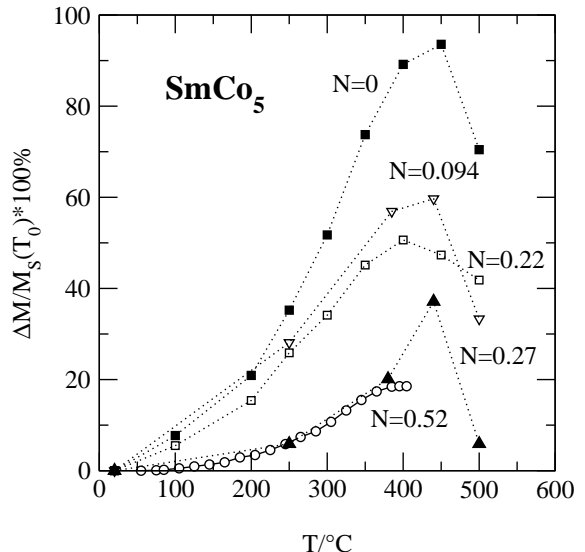


Figure 2: The TR for various $SmCo_5$ samples taken from Ref. [3] (squares) and Ref. [4] (triangles) and a VACOMAX 200 sample (circle) [16]. The data were transformed slightly from the original data to fit into the same plot. Also the demagnetization factors of the cylindrical samples were calculated from the geometry given by the authors. For details we refer to the original papers [3, 4].

saturation magnetization and the coercivity of that material. It can be seen from the curve for the $N=0.08$ sample that the TR survives in the region above the temperature T_{Hc} , where the coercivity vanishes, which is about 700 K. As we will see in the theory, this unexpected behavior can be ascribed to the fact, that the Curie temperature is more than 200 K higher than T_{Hc} . Lileev et. al. measured the TR for $SmCo_5$ samples with coercivities between $(0.35 \text{ T}/\mu_0$ and $3 \text{ T}/\mu_0$. They found that the inflection point, visible also in Fig. 3, vanishes for room temperature coercivities [17] below $1.6 \text{ T}/\mu_0$. For higher coercivities they found a decrease of the initial slope and an increase of the maximum of the TR with increasing coercivity. Measurements at samples, where the low-temperature coercivity was reduced by a special heat treatment [18] but otherwise prepared in the same way as the samples

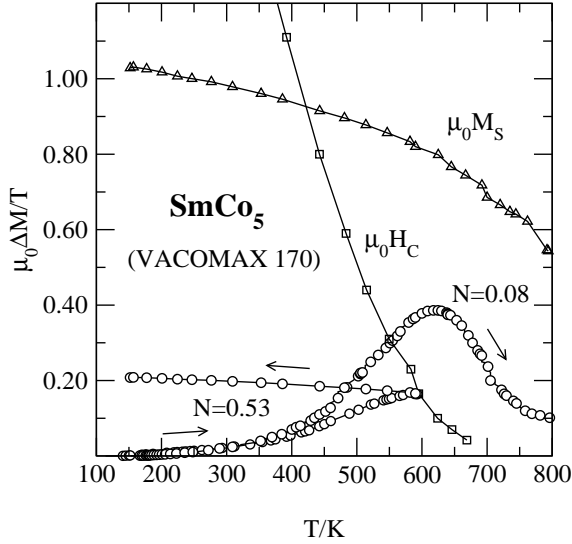


Figure 3: The temperature dependence of the coercivity H_C , saturation magnetization M_S and the TR for two samples of $SmCo_5$ with demagnetization factors $N=0.08$ and $N=0.53$ [16].

utilized in Fig. 3, did not show significant changes of the TR curves.

In contrast to $SmCo_5$, where the hysteresis mechanism is nucleation controlled, the coercivity of Sm_2Co_{17} magnets is caused by volume pinning of domain walls. For that behave a single phase solution of approximately 1:7 composition, i.e. slightly Co deficient with respect to Sm_2Co_{17} , is homogenized at approximately 1200 °C and afterwards cooled down to 800 °C, where it decays into the two adjacent stable phases by precipitation of $SmCo_5$ and $SmCu_5$. The contemporary commercial magnets of the 2:17 type are composed typically $Sm(Co,Fe,Cu,M)_7$, where the iron is used to increase the saturation magnetization and the other metals mainly for metallurgical reasons to obtain the precipitation microstructure. The latter is common to all Sm_2Co_{17} -magnets. The entirely different mechanism of magnetic hardening was the reason that in early years these compounds were believed not to show TR. Nevertheless a small TR is present also in Sm_2Co_{17} , as it is

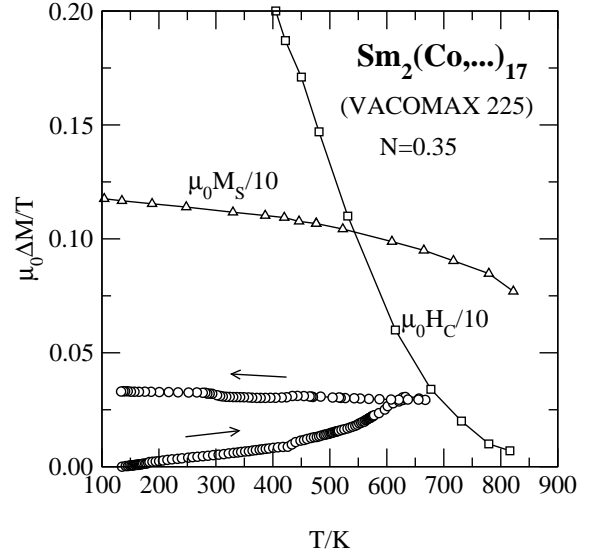


Figure 4: The temperature dependence of the coercivity H_C , saturation magnetization M_S and the TR for a Sm_2Co_{17} sample.

visible in Fig. 4. With regard to the smallness of the effect, which amounts to not more than 3%, it is not yet clear, whether the effect is characteristic for all Sm_2Co_{17} magnets or whether it is caused by imperfections of the microstructure, especially by the presence of a small content of $SmCo_5$ phase, as was argued in Ref. [13] in connection with the interpretation of virgin curves.

The $NdFeB$ -type magnets consist of the magnetic active phase $Nd_{2-x}Dy_xFe_{14}B$ surrounded by nonmagnetic phases. This guarantees for magnetic decoupling of neighboring grains. Within the main phase the nucleation mechanism was shown to control magnetization reversal [19]. Apart from the much lower Curie temperature and the spin reorientation below 137 K, the temperature dependence of coercivity and saturation magnetization is qualitatively the same as in $SmCo_5$ within the interesting temperature region, see Fig. 5. A remarkable difference is that coercivity and magnetization vanish nearly at the same temperature, i.e. at $T_{Hc} \approx T_C$. The observed TR, as depicted in Fig. 5, is considerably smaller

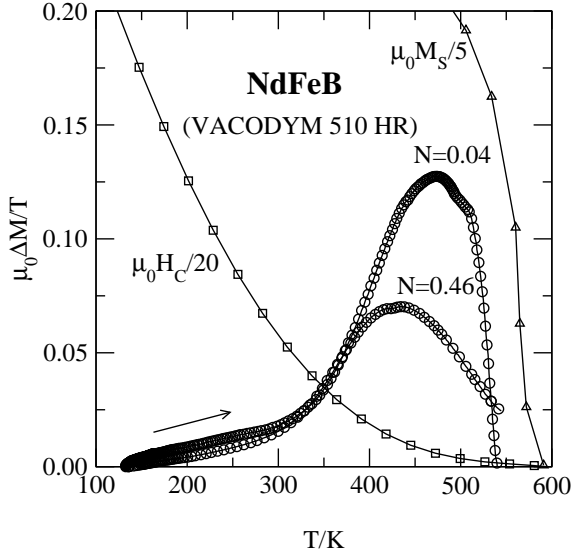


Figure 5: The temperature dependence of the coercivity H_C , saturation magnetization M_S and the ITR of two NdFeB samples with $N=0.04$ and $N=0.46$ resp. [16].

than in $SmCo_5$, but, with 12 % for the sample with very small demagnetization factor it is doubtless that it is an intrinsic characteristic of the magnet and can not be ascribed to imperfections in the microstructure. Livingston reported TR effects of 3% for rod samples ($N \approx 0.17$) with H_C about $1 \text{ T}/\mu_0$ and 24 % for a high coercive sample ($2.5 \text{ T}/\mu_0$) [5]. Furthermore, the low coercive samples were shown to contain a lot of multidomain grains in the dc-demagnetized state, in contrast to the high coercive specimen, which contained only a few. The same correlation between coercivity and TR was also reported in [11].

2.2 The ITR in Barium Ferrite

In comparison with the above mentioned intermetallic magnets the ceramic barium ferrite magnets exhibit a entirely different temperature dependence of the coercivity, as shown in Fig. 6. That is why the normal TR cannot be measured in this substances. Nevertheless an analogous experiment, where an initially saturated sample is dc-demagnetized

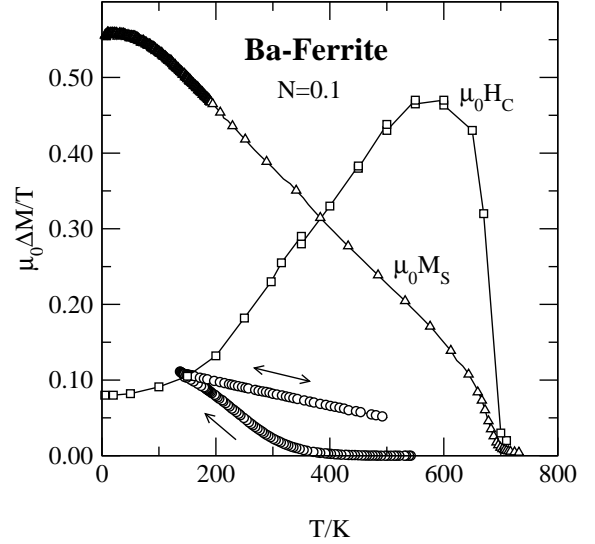


Figure 6: The temperature dependence of the coercivity H_C , saturation magnetization M_S and the ITR of a barium ferrite sample with $N=0.1$

at elevated temperature and afterwards cooled down, shows also a remarkable remagnetization [6]. This effect was called inverse thermal remagnetization (ITR). As seen from Fig. 7 we find again a strong dependence on the demagnetization factor. Since the coercivity upon cooling does not vanish one cannot observe a maximum. Instead one finds a plateau at lower temperature. Barium ferrite magnets are single-phased and the coercivity mechanism of barium ferrite is nucleation controlled. In that respect, apart from the different temperature dependence of the coercivity, the ITR of about 20% is similar to the TR in $SmCo_5$ -magnets.

2.3 The field dependence

The dramatic dependence of the TR on the demagnetization factor shows that a high sensitivity with regard to the internal magnetic fields is to expect. The influence of a small superimposed steady field was studied in [6, 20, 21]. To that behave the standard experiment was modified in the following way: After saturating the sample in a field of (about 10 T for $SmCo_5$ - and Sm_2Co_{17} -samples and about

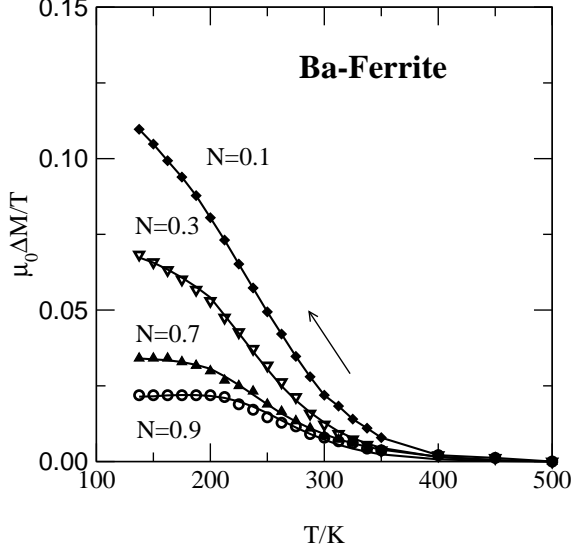


Figure 7: The ITR for four samples with $N=0.1$, $N=0.3$, $N=0.7$, and $N=0.9$ respectively. The solid lines are theoretical fits.

2 T for the barium ferrite samples) it was demagnetized by help of an opposite steady field $H_{ext}^{(1)}$. If this field equals the remanence coercivity H_R the magnetization will go to zero after switching off the field. Otherwise, if $H_{ext}^{(1)}$ deviates a little bit from H_R , the demagnetized state will be achieved on the recoil curve for a small negative residual field $H_{ext} < 0$, if $H_{ext}^{(1)}$ is greater than H_R , and for a small positive field otherwise, as the inset in Fig. 8 shows schematically. The field H_{ext} was then kept constant while the sample was heated (or cooled in the case of barium ferrite) and the resulting remanence enhancement $\Delta M(T)$ (TR-curve) was recorded. A set of such measured TR-curves (points) is given in Fig. 8 for $SmCo_5$ [22]. The initial temperature T_0 was 250 K. The solid lines are due to the theory, which will be explained below. The cases with $H_{ext} = 0$, i.e. $H_1 = -H_R$, correspond to a “normal” TR-curve. A systematic shift of the maximum temperature T_{max} , the maximum remanence enhancement ΔM_{max} and also of the initial slope $\Delta M_{TR}(T)/\Delta T$ [22] with increasing negative external field is observed. The same qualitative behavior can be measured in $NdFeB$ -

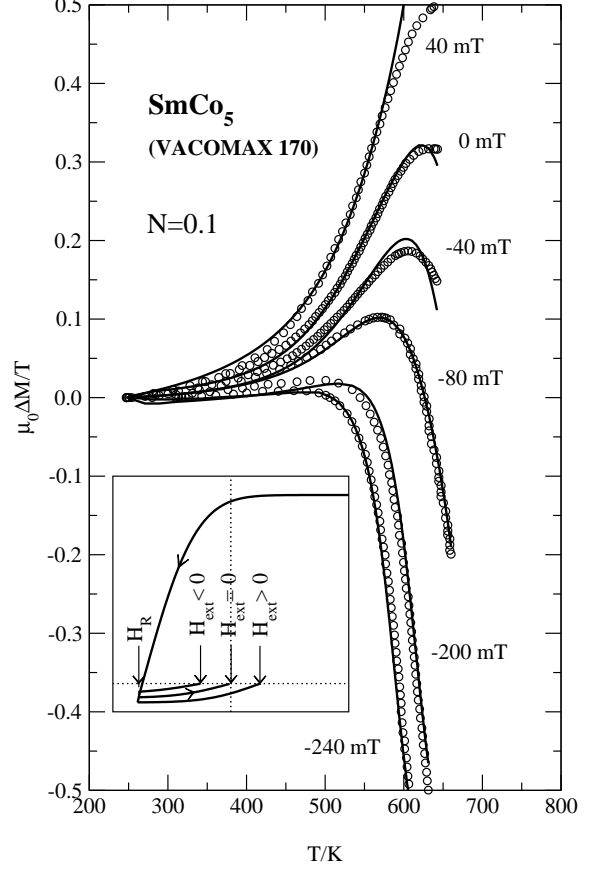


Figure 8: Measured TR-curves $\Delta M(T)$ (circles) for $SmCo_5$ [22] for different external steady fields applied during heating (small numbers at the curves). The solid lines are model calculations with parameters determined by the $H_{ext} = 0$ -curve (cf. section 3). The inset shows schematically how the initial state for the TR measurement is prepared.

magnets (Fig. 9) and Sm_2Co_{17} magnets (Fig. 10). Besides the fact, that the absolute TR-change with field is smaller in $NdFeB$ and even in Sm_2Co_{17} -samples, it looks very similar if the remanence-change with temperature is related to the remanence enhancement of the standard experiment [20]. Fig. 11 shows the analogous experiment for the ITR measured at a barium ferrite sample [23]. As it is obvious from the Figs. 8, 10, (for $NdFeB$ cf. [22]) a small positive field increases the TR extremely. Otherwise the TR may be suppressed at a cer-

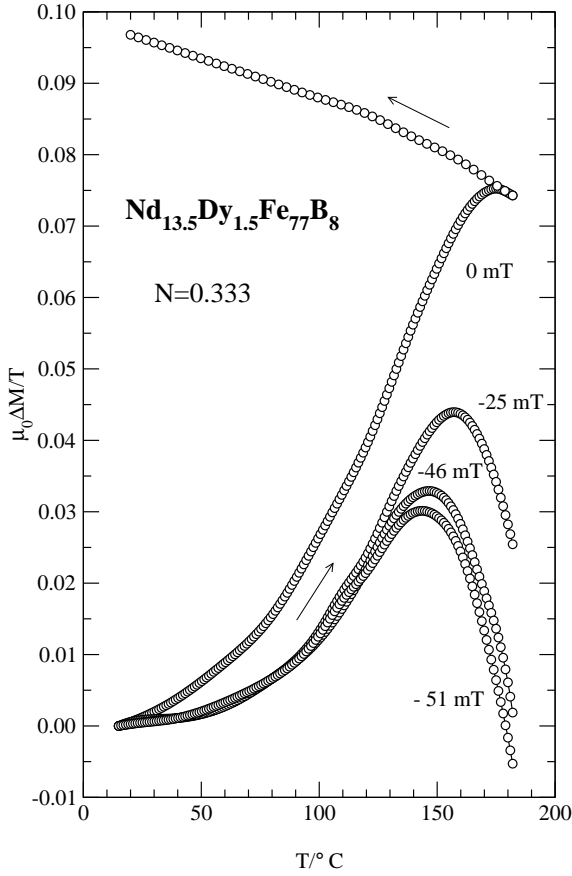


Figure 9: Measured TR-curves $\Delta M(T)$ (circles) for NdFeB for different external steady fields applied during heating (small numbers at the curves) [20].

tain negative field H' . The order of magnitude of this "suppression field" H' is to some extent a characteristic of the different types of permanent magnets [6, 20]. Fig. 12 extracts the maximum TR values in dependence of H_{ext} from Figs. 8, 9, 10, and 11. Comparing these results with other reported measurements one finds H' of the order of 200-500 mT for $SmCo_5$ [6, 20, 22] and 30-80 mT for $NdFeB$ -magnets [24, 22]. For $Sm_2(Co, \dots)_{17}$ -magnets this value seems to be more dependent on the chemical composition and technological treatment of the sample. Please note the mT-scale in the lower picture of Fig. 12 showing ΔM_{max} via H_{ext} data for Sm_2Co_{17} . Nevertheless H' is in the same region as in $SmCo_5$. This may support

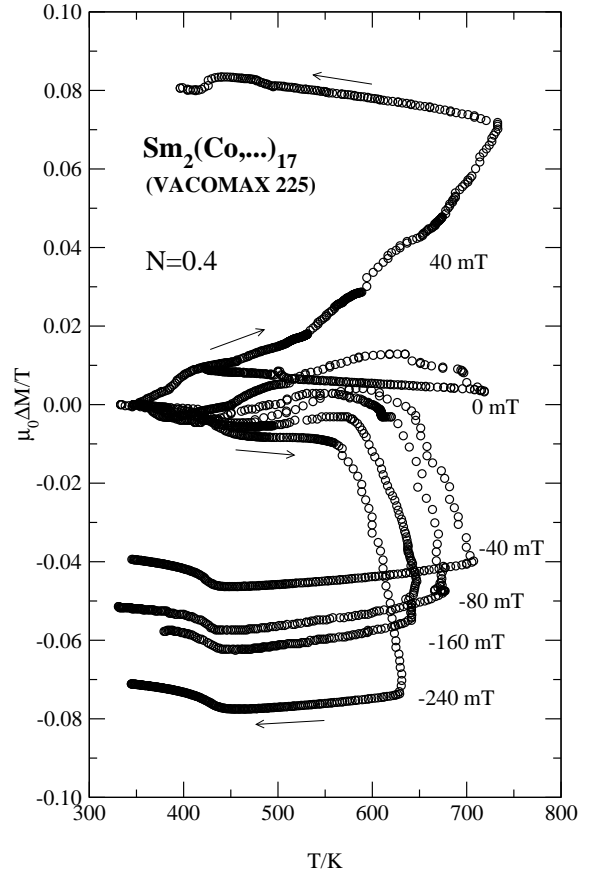


Figure 10: Measured TR-curves $\Delta M(T)$ (circles) for Sm_2Co_{17} for different external steady fields applied during heating and cooling resp. (small numbers at the curves).

the assumption that the TR in Sm_2Co_{17} is caused by a small amount of $SmCo_5$ grains as was proposed in [13]. The suppression field for the ITR in the barium ferrite sample of Fig. 11 is about 20 mT as may be seen from the filled squares in Fig. 12.

2.4 Influence of the initial temperature T_0

Ocularly the TR as well as the ITR are strongly connected with the temperature dependence of the coercivity. The difference of the coercivity $H_C(T_{max}) - H_C(T_0)$ is essentially for the TR. Thus the remanence increase should be depen-

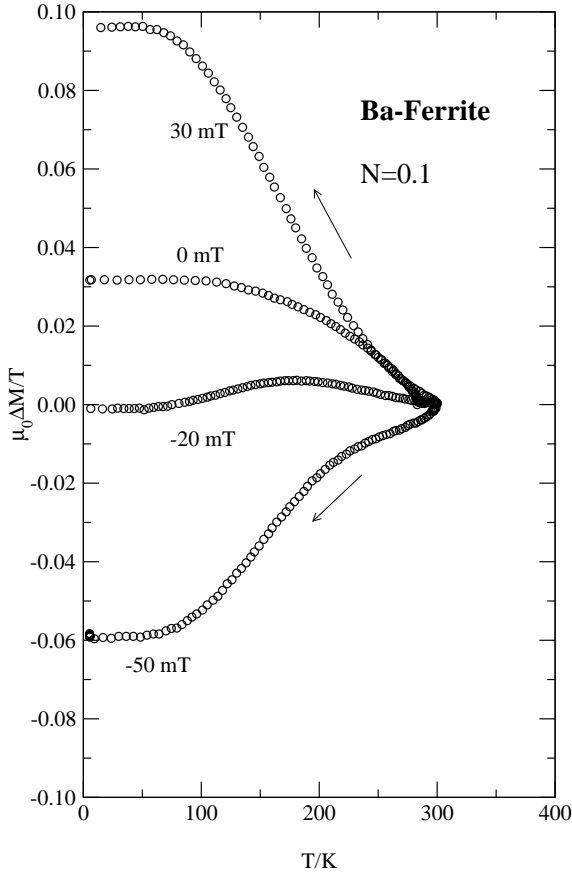


Figure 11: Measured ITR-curves $\Delta M(T)$ (circles) for barium ferrite for different external steady fields applied during cooling (small numbers at the curves) [23].

dent on the initial temperature T_0 as well. In Fig. 13, we show the results for oblate discs cut from a well aligned $SmCo_5$ -magnet (VACOMAX200). The upper part shows the initial irreversible TR at very low temperature, i.e. in the high coercive region, in detail, whereas the lower part shows the complete measurement to the maximum. Cooling down from the maximum the magnetization increases reversibly - exactly proportional to $M_S(T)$. More generally, if the TR experiment is interrupted at some temperature T_1 the magnetization change while cooling follows exactly $m_1 \times M_S(T)$, with m_1 being the ratio $\Delta M(T_1)/M_S(T_1)$, see e.g. Fig. 1 in [20]. On the one hand the amount of the TR is considerably influenced by a change

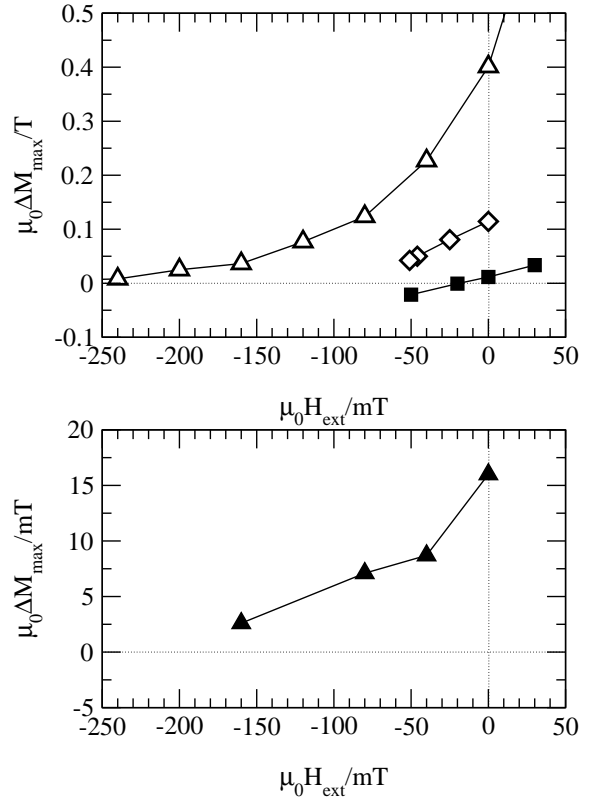


Figure 12: The maximum TR-curves in dependence of the superimposed magnetic field for the samples of Figs. 8, 9, 10, 11. Open triangles: $SmCo_5$, filled triangles: Sm_2Co_{17} , diamonds: $NdFeB$, squares: Barium Ferrite.

of the initial temperature, on the other hand only a small shift of the maximum position to lower temperatures is observed, if the initial temperature decreases. A likewise behavior is observed in $NdFeB$ as depicted in Fig. 14. Regarding the ITR in barium ferrite, where the initial temperature has to be chosen higher than the final temperature, we found again a strong dependence of the remanence increase on the initial temperature, whereas the region where the curves run into the plateau is slightly influenced only, as may be seen from Fig. 15.

2.5 Susceptibility and Repeating experiments

Since heat treatment is a mayor step in permanent-magnet production the possibility

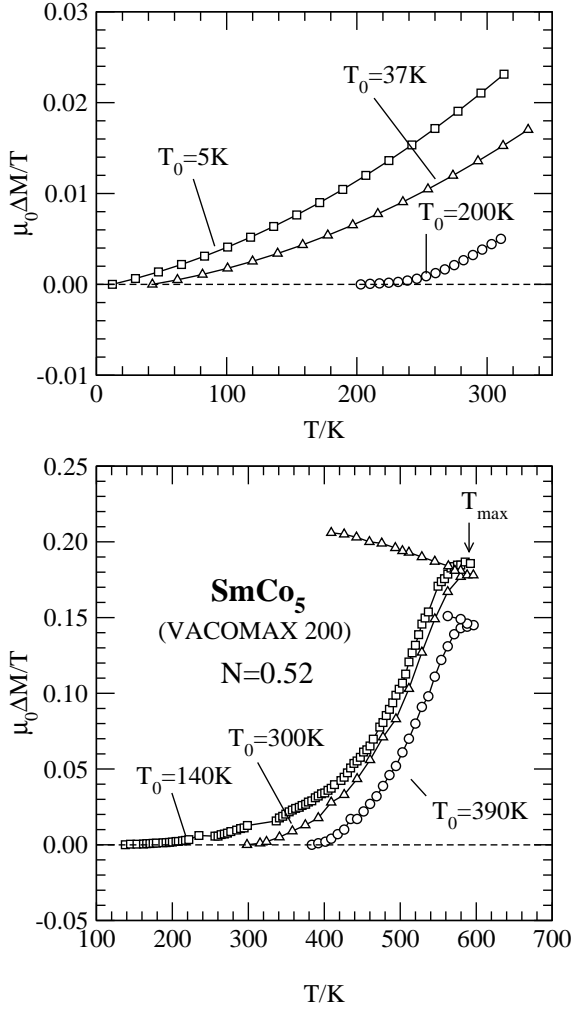


Figure 13: TR curves for different initial temperatures T_0 . The upper picture shows the initial TR for low initial temperatures.

is to envisage that the sample after the first TR experiment is irreversibly changed. This is of course of minor importance for the ceramic magnets but may be important in $SmCo_5$. Since the maximum temperature in $SmCo_5$ is about 600 K, it is low enough not to destroy the samples if the TR experiment does not last too long. In [4] the stability of the magnetization of $SmCo_5$ against thermal cycling between 20 °C and 75 °C was investigated. It was shown that it needs a few cycles to stabilize the magnetization change. For a sample which was partially dc-demagnetized (10% lowered remanence), it

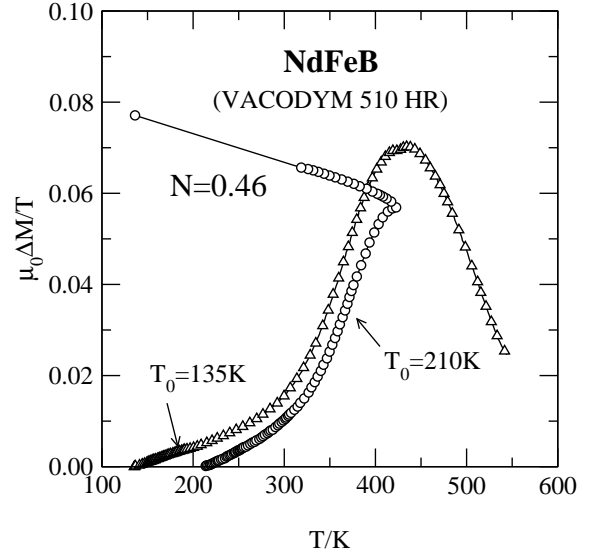


Figure 14: TR curves for two different initial temperatures for a NdFeB sample (NdFeB-HR 510) with $N=0.46$

was shown that 16 h annealing at 75 °C after ten cycles produces a sharp positive ΔM jump while additional hold of 38 h after cycle 13 produced no further significant change, besides a very small increase continuing up to 53 cycles. In [22] "repeating" experiments were reported, which differ a little bit from the thermal cycling procedure. Contrary to [4], where after every TR cycle the sample was saturated with a high field, the sample was dc-demagnetized from the remanent state which it reached after a cycle $T_0 \rightarrow T_{max} \rightarrow T_0$, i.e. without a new saturation. The idea behind this experiment was to prove the assumption, that the "hard grains", i.e. the fraction of grains which resist dc-demagnetization, are not concerned by the TR experiment. Fig. 16 shows a TR experiment together with its two repetitions. The difference between the curves are more likely due to the uncertainty in achievement of the dc-demagnetized state. Thus it is merely the "weak" grain fraction, which is switched both during dc-demagnetization and TR. After the first heating the sample is demagnetized by a much lower field, as may be seen from the inset of Fig 16, showing that the magnetic hard-

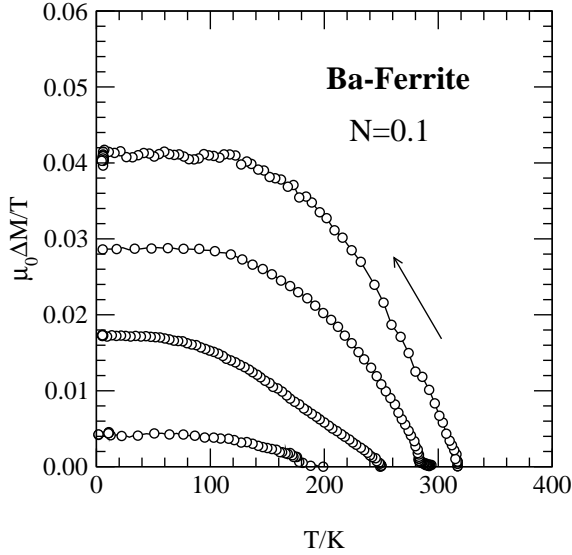


Figure 15: ITR curves for three initial temperatures for an isotropic sample.

ness of the weak grains was considerably lowered by heating to T_{max} . As a consequence an increase of the susceptibility is observed. In the experiment shown in Fig. 17 the TR curve was started as normal in the dc-demagnetized state, but a very small field of 10 mT was superimposed with alternating sign at every registration point of the magnetization. This results in a "normal" and two slightly shifted TR curves. The latter were taken as input for the calculation of the susceptibility χ , which was derived from the un-sheared susceptibility $\chi' = \Delta M / \Delta H_{ext}$ according to $\chi = \chi' / (1 - N\chi')$ with N being the demagnetization factor of the sample. The plot in Fig. 18 shows a continuous uprise with increasing temperature, which becomes very large beyond T_{max} . This sharp increase is due to the partial conversion of the weak grain fraction into the MDS and due to the lowering of their switching fields. This reduced coercivity of the weak grain fraction is frozen if the sample is cooled back to T_0 . Otherwise, the hard-grain fraction regains nearly reversibly its initial state, what means that the interaction field distribution due to the hard grains is re-established. In order to demagnetize the sample another time one has to over-

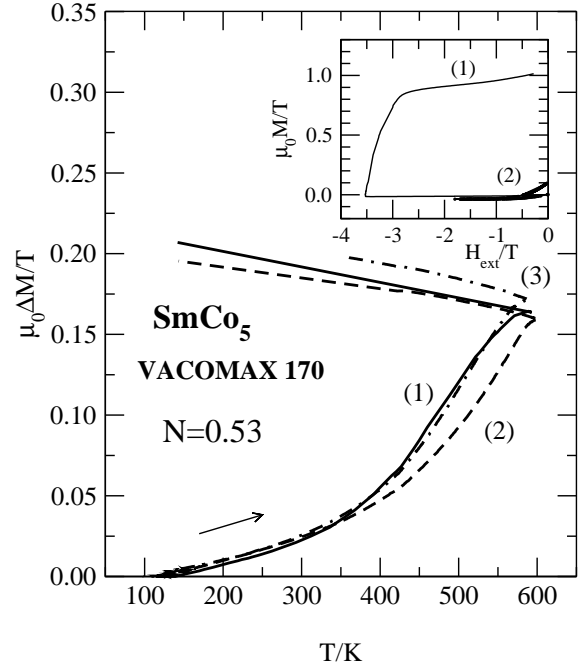


Figure 16: TR curve (1) and two repetitions (2,3) for the same sample of $SmCo_5$. The inset shows the dc-demagnetization curve for the first and second run.

come the smaller coercivity of the weak-grain fraction only. Afterwards the switched weak grains are located in nearly the same environment as before. As a consequence the TR is nearly the same in the repeating experiments.

2.6 Influence of texture.

Due to the technical importance, most of the reported TR experiments were done at well-textured samples. In Refs. [22, 25] TR investigation at isotropic magnets were reported. Comparing isotropic and well aligned samples of $SmCo_5$ one finds the same qualitative behaviour, but the TR of the isotropic specimen is reduced roughly four times with respect to the well aligned sample. Furthermore the difference of the TR curve and the first repetition differs a little bit more than in the well aligned material, as may be seen from Fig. 19 in comparison with Figs. 2,3, and 16. Qualitatively the same behavior was reported for

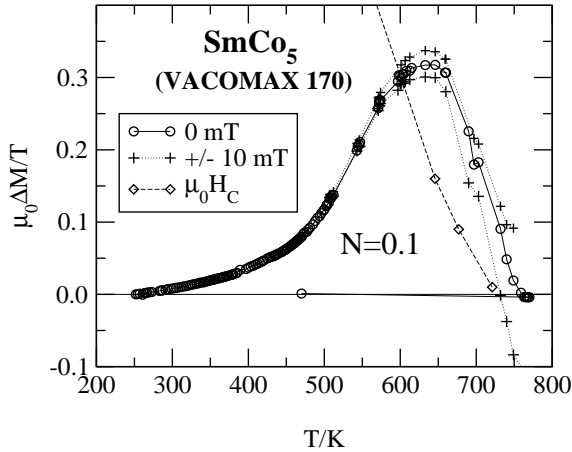


Figure 17: Measured TR curves for the same sample as in Fig. 8 for $\mu_0 H_{ext} = \pm 10 \text{ mT}$ (+). The circles represent the values measured for $\mu_0 H_{ext} = 0$. Furthermore the $H_C(T)$ is indicated.

isotropic sintered barium ferrite [25] Otherwise, an isotropic barium ferrite sample made from chemical precipitated 50 nm-powder, does not show any TR [6, 26]. To what extent this is connected with texture is not completely clear. The nano-sized grains are nearly Stoner-Wohlfarth particles, with an entire different coercivity mechanism [27]. Furthermore the density is much lower than in the sintered barium ferrite samples, what reduces the inter-grain interaction. That the latter plays an essential role can also be concluded from the experiments of Lileev and Steiner [7], who measured the initial TR for SmCo_5 in the temperature region from 4.2 K to 270 K for both well aligned sintered magnets and polymer-bounded samples with a SmCo_5 content of 20% and 80%. They found a considerable reduction of the TR with decreasing SmCo_5 packing density.

3 Theory

3.1 Early models

During the TR experiments the macroscopic magnetic energy is increased. This is only possible if the internal energy is considerably de-

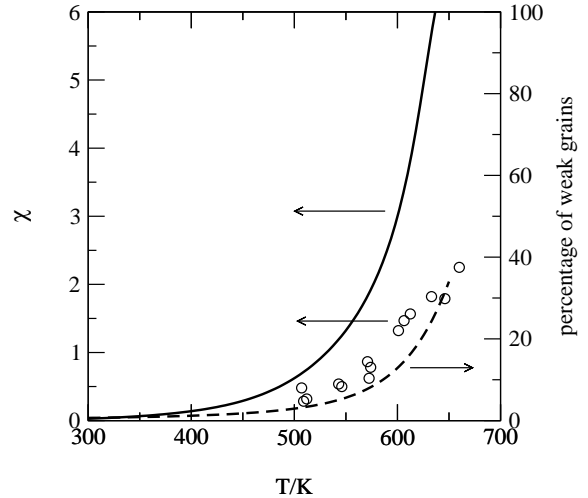


Figure 18: Measured and calculated susceptibility (solid line) $\mu_0 H_{ext} = \pm 10 \text{ mT}$ for the mCo_5 -magnet from Fig. 8. Furthermore the theoretically calculated percentage of “weak” grains is shown.

creased at the same time. During the initial dc-demagnetization process a state is prepared where one half of the grains is upwards (i.e. in the initial saturation direction) and the other half is downwards magnetized. Under the assumption that the intrinsic switching fields of the grains are not strong correlated with its position, we will find a extreme inhomogeneous magnetization at a microscopic scale in the dc-demagnetized state giving rise to considerable stray fields. While there is agreement that it is this part of the energy which governs TR, two different explanations for the mechanism behind TR were proposed. The first, introduced by Livingston [4], assumes that the downwards magnetized grains, which are in a single domain state before heating, decay into a multidomain state upon heating. This model got support from the direct observation of such grains in Kerr photographs taken from the surface of dc-demagnetized SmCo_5 -magnets [4] and NdFeB -magnets [5]. Although these intriguing observations make clear that to some extent nucleation of domain walls are involved in the TR, there are also some arguments against the

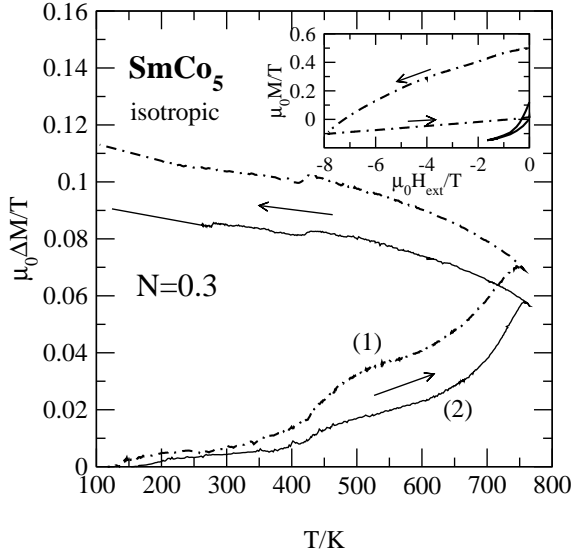


Figure 19: TR curve (1) and one repetition (2) for an isotropic sintered sample of $SmCo_5$ (Quality as VACOMAX 170, sintered and pressed without aligning field [18]). The inset shows the dc-demagnetization curve for the first and second run.

dominating role of the SDS-MDS mechanism. Without any calculations it is obvious that the maximum TR effect may not be greater than 50%, since after a complete decay of the weaker half only the harder grains contribute to the magnetization. This contradicts the observation of a much greater effect measured for $SmCo_5$ in a closed circuit [3]. Furthermore, the number of the multidomain grains seen in the shown Kerr photographs seems to be too low to explain the effect, despite the fact that it is not completely clear to what extent the surface observation is representative for the bulk behavior. The other model [6] assumed that the grain fraction with lower switching fields is first switched downward by the dc-demagnetization procedure. After taking away the external field they remain in a metastable state since their switching field is higher than the interaction field caused by the surrounding upwards oriented, i.e. harder magnetic, grains. Upon heating the switching fields are reduced and the weaker grains are switched

back in its initial direction. The decrease of the TR with decreasing filling factor [7] hints strongly at the role of inter-grain interaction. Further support of the interaction model got from the ITR in barium ferrite, since contrary to $SmCo_5$, Sm_2Co_{17} , and $NdFeB$, the low temperature minimum of the coercivity is still high enough to prevent a decay of grains into a multidomain state, thus the SDS-MDS mechanism can not explain the ITR. To clarify the role of multidomain grains Zaytzev et. al. [9] used Kerr micrography to count the number of multidomain grains in $SmCo_5$ magnets in the dc-demagnetized state at room temperature and at 120 °C. They demonstrated clearly that in the considered samples three processes contribute to the TR: Downward magnetized grains are either switched back or decay into the MDS under the influence of the interaction fields due to surrounding grains and in MDS grains the upward domains grow at cost of the downward domains. Besides the fact that the investigated samples exhibit a lowered coercivity and an unusual broad switching field distribution (SFD) in comparison with usual commercial magnets and that surface effects may result in a slight overestimation of the role of the MDS fraction from these experiments it becomes clear that a theoretical model has to describe both the interaction processes and the behavior of the MDS grains. It is interesting that they also observed hard grains changing from SDS to MDS. Whereas the theory presented below uses a phenomenological ansatz, Lileev et al. [17] presented a model based on simulations of interacting dipoles. This model, also taking into account the possibility of MDS states, was originally developed for the simulation of minor loops of permanent magnets [28]. By taking into account the temperature dependence of the model parameters it was also possible to simulate the TR. The shape of the only given curve deviates far from experiments. The authors see the reason for that in the mean-field treatment of the interaction contribution within their model. Whereas Monte-Carlo simulations allow to play with parameters it is al-

most impossible to determine parameters by fitting to the experiment. For that purpose a phenomenological description as given in the following seems more appropriate.

3.2 The inclusion model

The outlined theory was developed in Refs. [6, 10, 23, 29]. The poly-crystalline permanent magnet is an ensemble of high-coercive magnetic uniaxial grains. To fix our model we have to define the properties of both a single grain and the ensemble. For the single grain we assume that the temperature dependent saturation magnetization $M_S(T)$ should be known. Furthermore every grain should be characterized by its temperature dependent switching field $H_s(T)$, by its “internal” demagnetization factor n , by the direction of the easy axis due to the high uniaxial anisotropy \vec{c} , and by its volume V . Here $H_s(T)$ is the absolute value of the field needed for reversing the magnetization of the grain in a closed circuit. Regarding the ensemble we assume that all grains exhibit the same $M_S(T)$, that the easy axis \vec{c} of the grains are completely aligned, i.e. we restrict the model to ideally textured, single-phased magnets. These conditions are best fulfilled in $SmCo_5$ and barium ferrite magnets, whereas $NdFeB$ magnets contain more than one phase and Sm_2Co_{17} magnets show a precipitation structure resulting in a different switching behavior of a grain. Furthermore we allow that the grains differ in their switching fields H_s , but the distribution of these switching fields should be known. In non-interacting ensembles the switching field distribution may be determined from remanence measurements [30], but if the grains interact strongly this method fails. In Ref. [24] both the thermal remagnetization and the change of the H_s spectrum with increasing temperature of a $SmCo_5$ sample was measured, whereby the latter was approximately determined from dM/dH . This is justified if reversible magnetization processes are negligible as it is the case in $SmCo_5$ -magnets, For simplicity we assume a Gaussian normalized with

respect to the region $0 < H_s < \infty$ [10],

$$g(H_s) = \frac{2}{\sqrt{\pi}\sigma_s \left(1 + \operatorname{erf}\left(\frac{\bar{H}_s}{\sigma_s}\right)\right)} e^{-\left(\frac{H_s - \bar{H}_s}{\sigma_s}\right)^2} \quad (1)$$

with the “mean switching field” \bar{H}_s and the distribution width σ_s . The temperature dependence (not the absolute value!) of the switching fields of all grains are equal. For the moment we have to regard \bar{H}_s and σ_s as model parameters. Fortunately we will see later on that the theory delivers a possibility to relate \bar{H}_s to the coercivity H_C of the sample. A central point of TR is the treatment of the grain-grain interactions resulting in a collective behavior of adjacent grains. On a macroscopic length scale the internal magnetic fields and the magnetization of the sample are homogeneous. But, if the length scale is reduced to the order of some grain diameters the magnetization becomes coarser and the inhomogeneities gain influence. Averaging over volume elements containing a few grains only, yields values, which deviate from the average. Thus, we consider every grain as an inclusion embedded in a local environment, which may differ stochastically in its magnetic field and magnetization from the related averaged values. We show this schematically in Fig. 20. For simplicity we approximate the magnetization in the vicinity of the inclusion by the mean magnetization $\langle M \rangle$, neglecting the mentioned magnetization fluctuations. Otherwise we allow for field fluctuations $\Delta H = H - \langle H \rangle$ around the mean internal field in the environment of a grain. The mean internal field is related to the external applied field H_{ext} according to

$$\mu_0 \langle H \rangle = \mu_0 H_{ext} - N \langle M \rangle, \quad (2)$$

with N being the demagnetization factor of the sample. The field fluctuations are assumed to be Gauss distributed [10, 31],

$$f(H) = \frac{1}{\sqrt{\pi}\hat{\sigma}_f} e^{-\left(\frac{\Delta H}{\hat{\sigma}_f}\right)^2} \quad (3)$$

with $\Delta H = H - \langle H \rangle$.

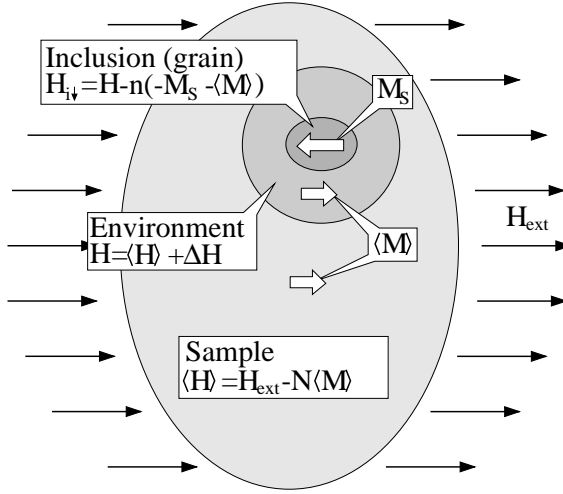


Figure 20: The grain is considered as an inclusion with magnetization $\pm M_S$ (here we assumed $-M_S$, symbolized by the long white arrow) embedded in an environment differing in its magnetic field H from the mean magnetfield $\langle H \rangle$ within the sample due to the fluctuation ΔH . Fluctuations of the magnetization in the environment are neglected, thus the magnetization in the environment is equal to the mean magnetization of the sample. This is symbolized by the two shorter white arrows of equal length.

what is a consequence of the central limit theorem of probability theory. Furthermore, the fluctuation width $\hat{\sigma}_f$ has to be an even function of the magnetization itself.

$$\hat{\sigma}_f = \sigma_f \xi(m) \quad \text{with} \quad m = \frac{\langle M \rangle}{M_S}. \quad (4)$$

This becomes obvious since in the saturated magnetized state the fluctuation width is zero (remember: ideal texture, all grains the same phase). Otherwise it is maximum for the dc-demagnetized state with random distribution of upward and downward magnetized grains. A Taylor expansion of $\hat{\sigma}_f(\langle M \rangle)$ to second order which fulfils these two boundary conditions yields

$$\xi(m) = (1 - m^2). \quad (5)$$

In general $\xi(m)$ depends on the correlation of neighboring grains. For instance the field of

a simple cubic array of uncorrelated dipoles, randomly oriented in $\pm z$ -direction, yields

$$\xi(m) = \sqrt{1 - m^2}. \quad (6)$$

Of course the local fields fluctuate around the mean internal field also in direction, thus, strictly speaking eq. (4) accounts for the fluctuations of the z -component only. Furthermore the deviation of the field direction from the easy axis gives rise to rotation processes, but this is surely a small effect in ideally aligned magnets with high anisotropy constants. In the early works on the TR theory a further point was stressed [6, 10, 17]: The field dependence of the switching field. This is indeed a crucial point, if one attempts to describe repeating experiments or the virgin curve, but can be neglected in the first TR experiment, if H_R is large enough to make most of the down-switched particles hard, as it seems to be the case in *SmCo₅* and barium ferrite. Taking into account this process is in principle not difficult, since it simply scales the SFD of the switched particles. This would introduce at least one additional parameter. We abstained from doing so by restricting the theory to the first TR run only.

3.3 Calculation of the Isothermal Demagnetization Curve

The first step is the calculation of the demagnetization curve from the saturated state down to the magnetic field $H_{ext}^{(1)}$ in the third quadrant. see Fig. 1. To save the opportunity to describe also the influence of a small steady field or a non-zero initial remanence on the TR we use a more general scheme of the TR experiment as shown in Fig. 21. After the saturation all grains are up (\uparrow) magnetized. They possess their maximum switching fields and $\langle M \rangle = M_S$ holds. If the external field is lowered to a value $H_{ext}^{(1)}$ (c.f. Fig. 21 the magnetization of a grain is switched down (\downarrow) if its internal field $H_{i,\uparrow}^{(1)}$ is lower than $-H_s$ and the internal field after switching $H_{i,\downarrow}^{(1)}$ will be smaller than $+H_s$. Thus

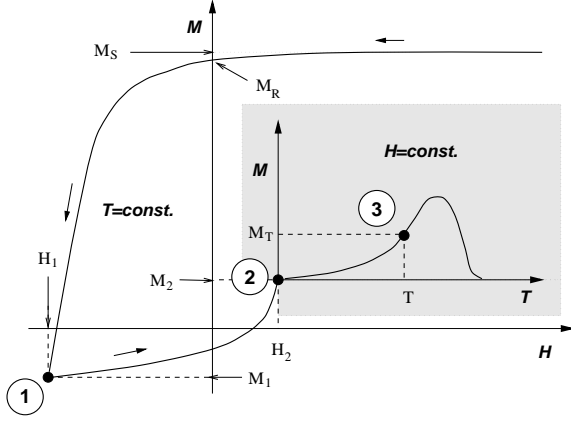


Figure 21: Generalized scheme of the a TR-Experiment: After saturation the sample is demagnetized isothermally by a steady field to an arbitrary point of the demagnetization curve, indicated by H_1 and M_1 . Afterwards the field is reduced to an arbitrary value H_2 . The related magnetization is M_2 . Finally the sample is heated (TR-Experiment) or cooled (ITR-Experiment) with the external magnetic field kept constant.

we have the two conditions

$$H_{i,\uparrow}^{(1)} < -H_s \quad \text{and} \quad H_{i,\downarrow}^{(1)} < +H_s \quad . \quad (7)$$

The internal fields before and after switching are with respect to the above introduced approximations

$$H_{i,\uparrow}^{(1)} = H - n(M_s - \langle M \rangle_1) \quad (8)$$

and

$$H_{i,\downarrow}^{(1)} = H - n(-M_s - \langle M \rangle_1) \quad (9)$$

Here H is the local field in the environment of the grain. A variation of the external field H_{ext} results in a change of $\langle M \rangle$ on the one hand and on the other hand it changes the probability $f(H)dH$ that the field in the environment of a grain is between H and $H + dH$ due to the relation (2) and eq. (4). If the first condition from eq. (7) is fulfilled but not the second, the grain cannot jump into a stable state. If the grain is large enough it solves the conflict by an incomplete jump, what turns its single-domain

state (SDS) into a multi-domain-state (MDS). We will call such grains “weak”. Whereas the “hard” grains can exist in states with $\pm M_S$ only, the magnetization of a weak grain $\langle M \rangle_i$ is an average over the upwards and downwards magnetized volume fractions within the grain. From phase theory of 180° -domains we get for the averaged magnetization of the i^{th} grain in dependence on the local field in the environment

$$\langle M \rangle_i = \langle M \rangle + \frac{H}{n} \quad . \quad (10)$$

Opposite to the hard grains the weak grains have no memory since the magnetization follows the local field immediately as long as $|\langle M \rangle_i| < M_S$ holds. Otherwise they are saturated up- or downwards. If one calculates the probability that a grain with a given H_s is in a MDS the switching condition (7) limits the integration over the local field distribution from above, whereas the back-switching condition $H_{i,\downarrow}^{(1)} > +H_s$ limits from below. The related probability is

$$p_w(H_s) = \int_{H_L}^{H_H} dH f(H) \quad (11)$$

with

$$H_H = -H_s + nM_S - n\langle M \rangle \quad (12)$$

$$H_L = H_s - nM_S - n\langle M \rangle \quad (13)$$

The requirement, that the upper limit has to be greater then the lower one, yields the condition $H_s < nM_s$. Thus, grains with switching fields smaller than their own internal demagnetizing field are weak. The magnetization of the volume fraction of the weak grains with a given H_s is

$$\begin{aligned} \langle M \rangle_w(H_s) = & M_S \int_{H_H}^{\infty} dH f(H) \\ & - M_S \int_{-\infty}^{H_L} dH f(H) \end{aligned}$$

$$+ \int_{H_L}^{H_H} dH f(H) \langle M \rangle_i. \quad (14)$$

The integral may be easily evaluated, where we have to take for the magnetic field $H_{ext}^{(1)}$ and the related magnetization $\langle M \rangle_1$ at the hysteresis curve. For hard grains H_L is higher than H_H . If these grains fulfill the switching condition, the second condition on eq (7) will be fulfilled automatically. The probability to find a grain downwards magnetized if a field $H_{ext}^{(1)}$ is applied is

$$p_1(H_s) = \int_{-\infty}^{+\infty} dH f_{(1)}(H) \times \\ \times \Theta(-H_s - H_{i,\uparrow}^{(1)}) \Theta(H_s - H_{i,\downarrow}^{(1)}), \quad (15)$$

with $H_{i,\uparrow}^{(1)}$ and $H_{i,\downarrow}^{(1)}$ being the fields within the grain in the upwards and downwards magnetized state resp. and $\Theta(x)$ is the Heaviside function. $f_{(1)}$ is the field distribution eq. (4) with $\langle H \rangle = H_{ext}^{(1)} - N\langle M \rangle_1$. After carrying out the integration in eq. (15) we get for the magnetization $\langle M \rangle_1 = M_S (1 - 2p_1(H_s))$ of a fraction of hard grains with a given H_s

$$\langle M \rangle_1(H_s) = -M_S \operatorname{erf}(x_H) \quad (16)$$

with

$$x_H = \frac{-H_s + nM_S - n\langle M \rangle_1 - H_{ext}^{(1)} + N\langle M \rangle_1}{\hat{\sigma}_f(m_1)}. \quad (17)$$

The total magnetization of the sample one gets from averaging with respect to H_s

$$\langle M \rangle_1 = \int_0^{nM_S} dH_s g(H_s) \langle M \rangle_{w,1}(H_s) \\ + \int_{nM_S}^{\infty} dH_s g(H_s) \langle M \rangle_1(H_s) \quad (18)$$

Here the integration has been split due to the different contributions of the weak and hard grains. For the weak grains we have to use eq.

(14). Since the right hand side of eq. (18) depends on the mean magnetization $\langle M \rangle_1$ itself, we have to solve this implicit equation numerically.

3.4 Calculation of the Isothermal Recoil Curve

Next, the external field is changed from $H_{ext}^{(1)}$ to $H_{ext}^{(2)}$ with $H_{ext}^{(2)} > H_{ext}^{(1)}$ via the recoil curve. Some of the hard “down”-grains are switched back, whereas the weak grains shift their magnetization reversibly. The related mean magnetization is $\langle M \rangle_2$. The contribution of the weak grains results from eq. (14), if we insert now $H_{ext}^{(2)}$ for H_{ext} and $\langle M \rangle_2$ for $\langle M \rangle$ resp. followed by an integration from zero to nM_S with respect to H_s . The contribution of the hard grains is more difficult to calculate, due to the memory effect. Let us consider the probability $w_{\downarrow\uparrow}(H_s)$ that a hard grain with a given H_s was switched by $H_{ext}^{(1)}$ and switched back by $H_{ext}^{(2)}$ afterwards. To calculate this probability it is inevitable to make an assumption on the correlation between the fluctuation of the local field H_1 which acts on a grain if $H_{ext}^{(1)}$ is applied and the fluctuation of H_2 according to the external field $H_{ext}^{(2)}$. Of course, if $H_{ext}^{(2)}$ is only slightly different from $H_{ext}^{(1)}$ it is unlikely that the neighborhood of a grain changes considerably, so that H_1 and H_2 should be strongly correlated. With increasing distance between $H_{ext}^{(1)}$ and $H_{ext}^{(2)}$ this correlation will vanish, due to the multitude of switching processes, hence we can average with respect to H_1 and H_2 independently, if the difference $H_{ext}^{(2)} - H_{ext}^{(1)}$ is not too small. Thus the probability $w_{\downarrow\uparrow}$ decouples accordingly $w_{\downarrow\uparrow}(H_s) = p_1(H_s)q_2(H_s)$ with $p_1(H_s)$ from eq. (15) and

$$q_2(H_s) = \int_{-\infty}^{\infty} dH f_{(2)}(H) \times \\ \times \Theta(H_{i,\downarrow}^{(2)} - H_s) \Theta(H_{i,\uparrow}^{(2)} + H_s) \\ = \frac{1}{2} \left(1 - \operatorname{erf}(y_L) \right) \quad (19)$$

with

$$y_L = \frac{H_s - nM_s - n\langle M \rangle_2 - H_{ext}^{(2)} + N\langle M \rangle_2}{\hat{\sigma}_f(m)}. \quad (20)$$

Due to the mentioned magnetization changes in the environment of a grain it may happen that grains which resisted $H_{ext}^{(1)}$ are switched down by $H_{ext}^{(2)}$ (“up”-“down”-contribution). The related probability factors also

$$w_{\uparrow\downarrow}(H_s) = (1 - p_1(H_s)) p_2(H_s) \quad (21)$$

with $p_1(H_s)$ again from eq. (15) and

$$\begin{aligned} p_2(H_s) &= \int_{-\infty}^{\infty} dH f_{(2)}(H) \times \\ &\quad \times \Theta(-H_s - H_{i,\uparrow}^{(2)}) \Theta(H_s - H_{i,\downarrow}^{(2)}) \\ &= \frac{1}{2} \left(1 + \operatorname{erf}(z_H) \right) \end{aligned} \quad (22)$$

with

$$z_H = \frac{-H_s + nM_s - n\langle M \rangle_2 - H_{ext}^{(2)} + N\langle M \rangle_2}{\hat{\sigma}_f(m)}. \quad (23)$$

There are two further probabilities corresponding to the remaining two histories, which a grain may experience, i.e. the probability that it resisted both $H_{ext}^{(1)}$ and $H_{ext}^{(2)}$ (“up”-“up” contribution) and the probability that a grain was switched by $H_{ext}^{(1)}$ but resisted back-switching by $H_{ext}^{(2)}$ (“down”-“down” contribution). We find

$$w_{\uparrow\uparrow}(H_s) = (1 - p_1(H_s)) (1 - p_2(H_s)) \quad (24)$$

and

$$w_{\downarrow\downarrow}(H_s) = p_1(H_s) (1 - q_2(H_s)). \quad (25)$$

Thus hard grains with a given H_s contribute to the magnetization

$$\begin{aligned} M_2(H_s) &= M_s \left(w_{\uparrow\uparrow}(H_s) - w_{\uparrow\downarrow}(H_s) \right. \\ &\quad \left. + w_{\downarrow\uparrow}(H_s) - w_{\downarrow\downarrow}(H_s) \right). \end{aligned} \quad (26)$$

Averaging with respect to H_s yields the recoil curve for the mean magnetization $\langle M \rangle_2$ in dependence on both magnetic fields $H_{ext}^{(1)}$ and $H_{ext}^{(2)}$.

$$\begin{aligned} \langle M \rangle_2 &= \int_0^{nM_S} dH_s g(H_s) \langle M \rangle_{w,2}(H_s) \\ &\quad + \int_{nM_S}^{\infty} dH_s g(H_s) \langle M \rangle_2(H_s). \end{aligned} \quad (27)$$

3.5 Calculation of the (Inverse) Thermal Remagnetization

The above calculation of the demagnetization and the recoil curves was done with the implicit understanding that the magnetization changes isothermally at a temperature T_0 . The actual TR (ITR) occurs if a dc-demagnetized magnet is heated (cooled) while $H_{ext}^{(2)}$ is kept constant. Changing the temperature has two effects. On the one hand the saturation magnetization decreases with increasing temperature and on the other hand the switching fields H_s are changed. Whereas the temperature dependence of the saturation magnetization can be measured easily, it is impossible to measure it for the switching fields. Fortunately, one can solve eq. (14) for \bar{H}_s with $H_{ext}^{(1)} = H_C$ and $\langle M \rangle_1 = 0$ [23]. $H_C(T)$ and $M_S(T)$ are taken from measurements. If the influence of the weak grains is negligible, $\bar{H}_s(T)$ is related to $H_C(T)$ and $M_S(T)$ by the simple formula $\mu_0 \bar{H}_s(T) = \mu_0 H_C(T) + nM_S(T)$ [23]. Furthermore we adopt the temperature dependence of \bar{H}_s for arbitrary values of the switching fields, i.e

$$H_s(T) = H_s(T_0) \times (\bar{H}_s(T)/\bar{H}_s(T_0)). \quad (28)$$

The calculation of the magnetization $\langle M \rangle_2^T$ at an enhanced temperature T is similar to the calculation of the magnetization $\langle M \rangle_2$ by help of eq. (28), whereby the temperature induced deformation of the switching field distribution has to be regarded. Due to the assumption on

$H_s(T)$ and the normalization of the switching field distribution follows that σ_s has the same temperature dependence like $H_s(T)$. The magnetization of a weak grain with given H_s at the temperature T results from eq. (14) with the appropriate $H_s(T)$, $M_S(T)$, and $\langle M \rangle_2^T$ inserted. For the hard-grain contribution we have to calculate the probabilities $w_{\uparrow\uparrow}$, $w_{\uparrow\downarrow}$, $w_{\downarrow\uparrow}$, and $w_{\downarrow\downarrow}$, however for the increased (lowered in case of ITR) temperature T . We find for the magnetization of the hard-grain fraction with given H_s

$$M_2^T(H_s) = M_S^T \left(w_{\uparrow\uparrow}^T(H_s) - w_{\uparrow\downarrow}^T(H_s) + w_{\downarrow\uparrow}^T(H_s) - w_{\downarrow\downarrow}^T(H_s) \right). \quad (29)$$

It is obvious that the probability $p_1(H_s)$ remains unchanged, since the grains were switched downwards at the initial temperature T_0 . Therefore we have

$$w_{\uparrow\uparrow}^T(H_s) = \left(1 - p_1(H_s)\right) \left(1 - p_2^T(H_s)\right) \quad (30)$$

$$w_{\uparrow\downarrow}^T(H_s) = \left(1 - p_1(H_s)\right) p_2^T(H_s), \quad (31)$$

$$w_{\downarrow\uparrow}^T(H_s) = p_1(H_s) q_2^T(H_s), \quad (32)$$

$$w_{\downarrow\downarrow}^T(H_s) = p_1(H_s) \left(1 - q_2^T(H_s)\right). \quad (33)$$

The probabilities $q_2^T(H_s)$ and $p_2^T(H_s)$ become temperature dependent both directly due to $H_s(T)$, $M_S(T)$, and $\sigma_f(T)$ and indirectly via $\langle M \rangle_2^T$. The temperature dependence of $\sigma_f(T)$ was assumed to be that of M_S , since the fluctuations are caused by the inhomogeneities of the magnetization. Finally the TR or the ITR can be calculated from the following implicit self-consistent equation

$$\begin{aligned} \langle M \rangle_2^T &= \int_0^{nM_S} dH_s g(H_s) \langle M \rangle_{w,2}^T(H_s) \\ &+ \int_{nM_S}^{\infty} dH_s g(H_s) \langle M \rangle_2^T(H_s). \end{aligned} \quad (34)$$

3.6 Influence of approximations

The theory teaches us, which processes are necessary to describe different parts of the TR

curve qualitatively right. In order to describe a residual remanence beyond T_{Hc} , $H_S(T)$ has to be determined self-consistently from $H_C(T)$ and $M_S(T)$. In Fig. 22 we study different

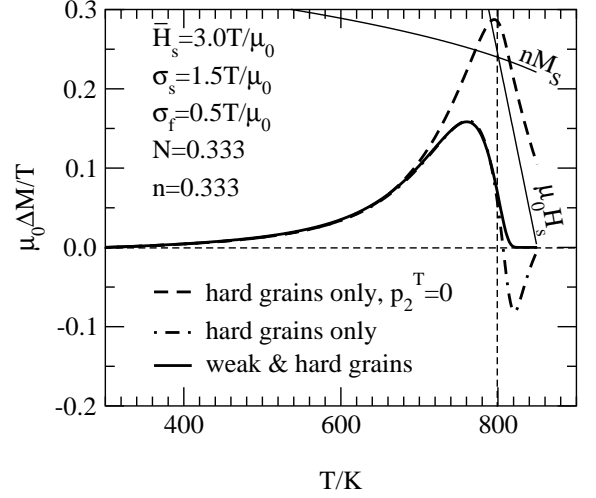


Figure 22: The TR for different levels of approximation. The solid line gives the results of the presented theory. The dot-dashed line results from neglecting the weak grain fraction and for the calculation of the dashed line, both the weak grains and p_2^T , i.e. the probability, that a grain which resisted $H_{ext}^{(1)}$ will be switched while heating at $H_{ext}^{(2)} = 0$, were neglected.

approximation levels. The influence of weak grains is small as long as the temperature is below T_{max} . For $T > T_{max}$ the neglect of the weak grains would result in a qualitative different behaviour, since we get a sign change of the TR before it finally vanishes, as shown in Fig. 22 in dashed-dotted manner. The reason for that peculiarity is made clear in Fig. 23, where we have plotted the temperature dependence of the probabilities $w_{\uparrow\uparrow}$, $w_{\uparrow\downarrow}$, $w_{\downarrow\uparrow}$, and $w_{\downarrow\downarrow}$ regarding the hard grain fraction. It is obvious that at first $w_{\downarrow\uparrow}$ increases and when it drops down $w_{\uparrow\downarrow}$ rises up, thus explaining the sign change. This behaviour is not observed if the probability p_2 , i.e. that a grain which resisted $H_{ext}^{(1)}$ will be switched by $H_{ext}^{(2)}$, is neglected, as it was done in former theories,

but then an overestimation of the TR occurs, as visible in Fig. 22. For the description of the TR at higher temperatures it is necessary to take into account, that above T_{max} even the switching fields of the hardest grains are lowered enough to be switched by the still existing stray fields. The latter do not vanish until the magnetization breaks down. It is

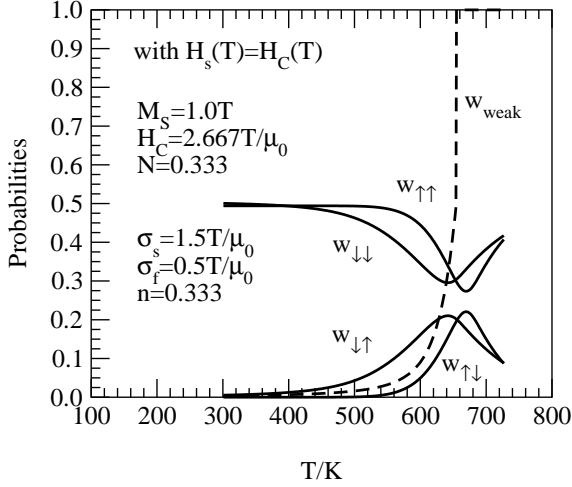


Figure 23: The probabilities $w_{\uparrow\uparrow}^T$, $w_{\uparrow\downarrow}^T$, $w_{\downarrow\uparrow}^T$, and $w_{\downarrow\downarrow}^T$ (cf. eqs. (30-33)) in dependence on the temperature. The dashed line shows the ratio of the volume of weak grains to the total volume.

worth to point out, that weak grains are not necessary to get effects of more than 50 %. Such a large TR one gets due to the feedback of the magnetization via the internal demagnetizing fields. In some sense this models the well known avalanche effects observed during hysteresis measurement, which should also occur to a certain extent if the sample remagnetizes.

In the early works on the TR a further point was stressed [6, 10, 17]: The field dependence of switching field. This is a crucial point, if one attempts to describe repeating experiments or the virgin curve, but can be neglected in the first TR experiment, if $H_{ext}^{(1)}$ is large enough to make most of the down-switched particles hard, as it seems to be the case in $SmCo_5$ and

barium ferrite. Taking into account this process is in principle not difficult, since it simply scales the SFD of the switched particles. This would introduce at least one additional parameter. We abstained from doing so by restricting the theory to the first TR run only. Taking into account all probabilities and weak grains the model describes the TR dependence on the demagnetization factor N of the sample and the initial temperature T_0 well, as was shown in Ref. [23] for the TR and in Ref. [29] for the ITR. In the following we concentrate on the investigation of the influence of internal model parameters.

3.7 Comparison to the experiment

The limitations of the presented model, i.e. the assumed perfect texture and single phase consistency, are best fulfilled in well aligned $SmCo_5$ - and barium ferrite magnets. There are three unknown parameters of the theory n , σ_f and σ_s which have to be determined by adjusting the theory to the experiment. Fig.

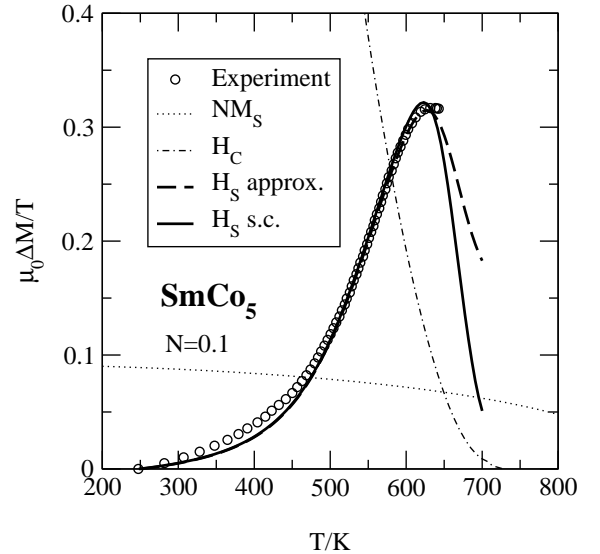


Figure 24: Comparison of the best-fits for the $SmCo_5$ sample from Fig. 8 with $H_s(T)$ calculated self-consistently (solid line) and approximately (broken line) from $H_c(T)$ and $M_s(T)$.

24 shows the best fit results for the $SmCo_5$

sample with $N=0.1$ used in Fig. 8 where the (smoothed) measured temperature dependence of H_C and M_S (shown in Fig. 3) was used as input. The best agreement is achieved, if $H_S(T)$ is calculated self-consistently from eq. (18). Although up to the maximum the difference is negligible the approximated formula fails at higher temperatures where most of the grains are weak. Furthermore the influence of the form of the m -dependence of $\hat{\sigma}_f$ was checked. It comes out that the initial slope is a little bit increased and the maximum becomes a little bit lower and broader if the function $\hat{\sigma}_f(m)$ is chosen wider. Unfortunately these changes are to less in comparison with the inaccuracies of the present experimental data that a definite decision can not be made.

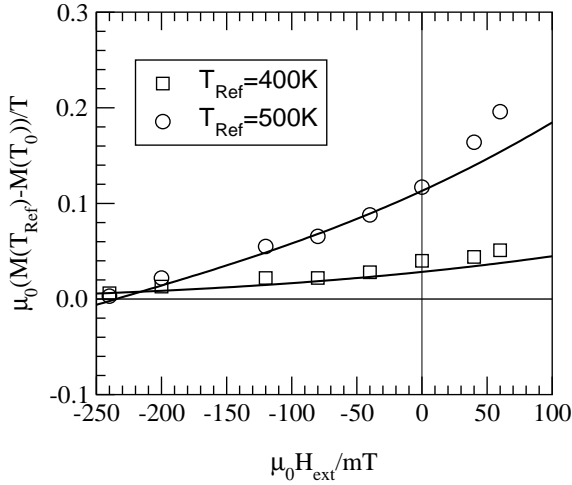


Figure 25: Calculated TR between T_0 and two reference temperatures T_{ref} in dependence on a small steady field applied while heating (solid lines). The circles and squares are experimental points taken from Fig. 8.

Figs. 8 and 25 relate the theory to the experiment. For that the parameters were determined by fitting the standard experiment, i.e. with $H_{ext}^{(2)} = 0$. The graphs for the other values of $H_{ext}^{(2)} \neq 0$ were then calculated (not fitted!) with the same parameter set. The agreement is fairly well. Of course, it can be made perfect by fitting the parameter for every curve

separately. The variation of the parameters, given in Tab. 2, shows that the minima in the least-square sum are rather flat and that the fit data have to be taken as rough estimates. From

H_{ext}/mT	$\mu_0\sigma_s/T$	$\mu_0\sigma_f/T$	n
VACOMAX 170 $N=0.1$			
+40	2.526	0.360	0.299
0	1.503	0.467	0.349
-40	2.324	0.324	0.256
-80	1.709	0.417	0.298
-120	2.200	0.407	0.268
-240	1.639	0.421	0.427
VACOMAX 200 $N=0.53$			
0	1.60	0.91	0.56

Table 2: The best-fit values for a VACOMAX 170 sample, determined from the experimental curves given in Fig. 8 and for VACOMAX 200 sample [16].

comparing the curves with other samples of the same material and by calculating the N - and T_0 -dependence with the values given above we found the fit parameters belonging to $H_{ext} = 0$ to be the most reliable ones. In Fig. 26 the theoretical curves are calculated in analogy to the measurements presented in Fig. 17. From

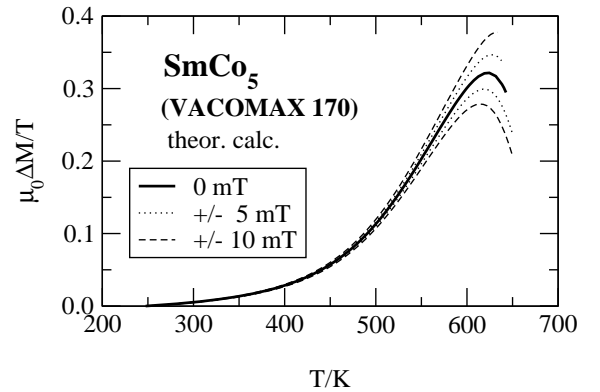


Figure 26: Calculation of the influence of a small external field variation. Solid line: Best-fit TR curve for the same sample as in Fig. 8. Dotted Line: Calculation for $\mu_0 H_{ext} = \pm 5 \text{ mT}$. Broken Line: Calculation for a for $\mu_0 H_{ext} = \pm 10 \text{ mT}$.

the comparison of both figures the qualitative agreement is ocularly, but the calculated susceptibility is higher than the measured, what may be caused by the model assumption of ideal mobility of the domain walls within the weak grains. A further reason is the existence of a small volume fraction of lower coercivity components, which results in a small dip of the demagnetization curve, i.e. in a second broad flat peak of the H_s distribution, which is not altered with temperature [24]. That weak grains are responsible for the susceptibility enhancement becomes clear if one calculates the number of weak grains in dependence on the temperature (dotted line in Fig. 18). For the ITR in barium ferrite multi-domain grains are of less importance, since upon cooling the coercivity is not reduced below nM_S if n is small. Thus most of the grains remain in SDS. Again we find an excellent agreement of the fitted curve with the experimental values, as may be seen from Fig. 7. From Tab. 3 The agreement is

sample	N	σ_s/T	σ_f/T	n
B1	0.1	.124	.128	.156
B2	0.1	.124	.129	.156
B3	0.3	.120	.106	.153
B4	0.7	.131	.086	.067
B5	0.9	.102	.113	.049

Table 3: Best fit values for the barium ferrite samples from Fig. 6 (B1) and Fig. 7 (B2-B5).

much better for the elongated samples, whereas for the prolate discs internal deviations from the assumed uniform magnetization seem to be more important [32]. In Fig. 27 the calculated field dependence of the maximum TR for sample B1 is shown, where the fit values from Tab. 3 have been used.

The influence of the intrinsic model parameters σ_s , σ_f and n on the TR is studied in Fig. 28 for model parameters taken from Tab. 2. The most interesting features are the strong dependence on the field fluctuation width σ_f and on the internal demagnetization factor n .

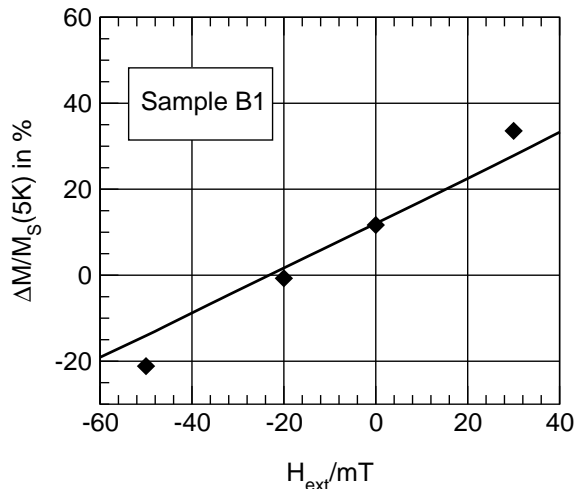


Figure 27: Comparison of the calculated (solid line) and measured (diamonds) dependence of the ITR in barium ferrite on a small steady field applied while cooling from 300 K down to 5 K.

For small internal demagnetization factors, i.e. for elongated grains, the TR is small, whereas effects up to 100 % are possible for platelet-shaped grains. This corresponds well with the simulation results of Ref. [33]. The shift of the TR peak to higher temperatures as well as the sharpening with decreasing fluctuation width can be understood easily from the fact that the switching field of a volume fraction with given H_s has to be reduced more by temperature before it contributes to the TR. Taking into account the different temperature dependence of H_C the same may be said for the ITR in barium ferrite, as seen in Fig. 29.

4 Discussion

Summarizing the experimental facts we find that TR or ITR is observed in all technical relevant permanent magnetic materials. Regarding the prerequisites for TR and ITR we found that a necessary condition for the effect is the preparation of an asymmetrical demagnetized initial state, where the average switching field of positively and negatively magnetized grains is different. A further

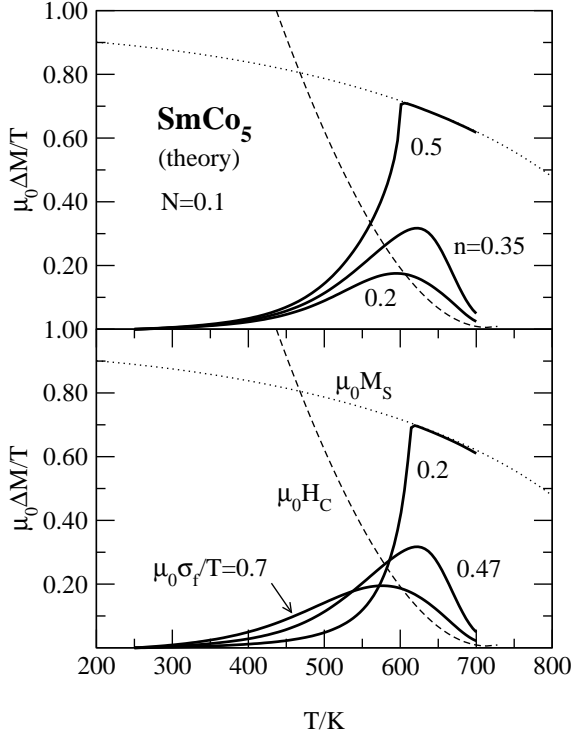


Figure 28: Calculation of the influence of σ_f and n on the TR. The other parameters are the best-fit values from Tab. 2

condition is the existence of a sufficient broad distribution of field fluctuations. Furthermore the reduction of the coercivity with temperature has to be large enough, that the interaction fields may overcome the switching fields. The sign of the temperature coefficient of coercivity determines whether normal TR or ITR happens. Some features are common to all the four considered groups of permanent magnets (i) the strong dependence on the demagnetization factor N of the sample (ii) the extreme sensibility against a small superimposed steady-field H' (iii) the strong dependence on the initial temperature T_0 (iv) the increase of the susceptibility after a TR cycle and (v) the reproducibility of TR in "repeating experiments". Otherwise, looking in detail, every permanent magnetic material shows some individual characteristics. For the $SmCo_5$ magnets it is mainly the survival of a TR effect beyond the temperature T_{Hc} ,

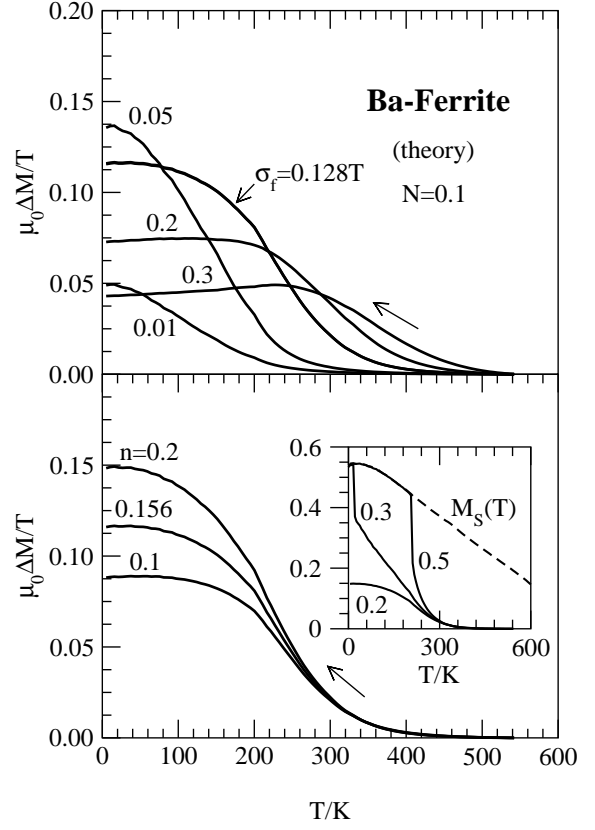


Figure 29: Calculation of the influence of n and σ_f on the ITR. For the other parameters the best-fit values for sample B1 from Tab. 3 were used.

due to the big difference $T_C - T_{Hc}$. For the $NdFeB$ magnets it is the very small switching field distribution and the decoupling of the magnetic active grains which reduce the effect. The peculiarities of the barium ferrite magnets are caused by the different temperature dependence of the coercivity. The Sm_2Co_{17} -type magnets differ from all the others by the underlying coercivity mechanism of the main magnetic phase. Regarding the latter materials, it is undoubtedly that the samples, where measurements were published, exhibit TR with all the main features. Otherwise the magnitude of the effect is so small, that it is at present impossible to decide, whether pinning controlled magnets really show TR. Moreover, also within a given material group, samples produced with different technologies may differ

considerably in the amount of TR.

Nevertheless most of the observed features can be well understood in the framework of the above presented theory, at least qualitatively, if it is possible to estimate how the special characteristics of a material are reflected in the model parameters. The latter are mainly the internal demagnetization factor n and the width of the field fluctuation σ_f . The parameter σ_s results from the assumption of a gaussian SFD, which was introduced for simplicity. This simplification is of less importance if one calculates the TR, since it is very sensitive to field fluctuations but less sensitive to the SFD. For the hysteresis curve the situation is vice versa. Thus a single gaussian may not be accurate enough to fit the hysteresis curve in good quality. In principle this situation may be improved by calculating a more realistic SFD from the measured hysteresis curve. Regarding the calculation of the TR this would result in substituting the erf-function by the adequate primitive of the SFD. We do not think that this is the main point, instead we regard the simple version of the "inclusion approximation" (for details see [23]) as the most problematic approximation, since it describes the retroaction of the different environments onto the different grains by only one parameter, the internal demagnetization factor n . An argument in favour of this approximation is the fact, that it yields exactly the same relation between the coercivity and the related (averaged) switching field as introduced both empirically [34] and theoretically [35]. Through this paper we used the term "grain" for the magnetic bistable units for simplicity. Indeed, these magnetic units may be different from the crystallites. Especially if there are strong interactions between the grains, it may be that some grains agglomerate and switch coherently. For instance the small internal demagnetization factor n in the above cited barium ferrite samples shows that the magnetic units are elongated, so it seems possible, that short chains of crystallites play the role of the magnetic units. The other ap-

proximations are of less importance. Of course, the magnetic field fluctuates in three dimensions regardless of the assumed ideal texture, but, in the case of strong anisotropy it is merely the z-component of the field which switches the grains, and these fluctuations will be Gaussian again and are therefore contained in the model. The latter is supported by the TR and ITR experiments at isotropic sintered samples of $SmCo_5$ and barium ferrite. Both the remanence and the z-component of the fluctuating fields are reduced by a factor two with respect to the aligned samples, This yields approximately the observed factor four for the reduction of the TR and ITR resp.. The theory works best for the well textured $SmCo_5$ - and barium ferrite samples. For $NdFeB$, albeit curves may be fitted as well, the meaning of the fit parameters is not as clear. The existence of nonmagnetic phases will reduce the effective magnetization, i.e. the magnetic units may be thought as a composition of a magnetic nucleus surrounded by a small nonmagnetic layer [19]. Thus the mean field can vary between $\pm cM_S$, with c being the content of magnetic phases, whereas in the switching conditions, it must be taken into account, that the switching unit is the magnetic nucleus only. Furthermore, the normalization of the SFD has to be changed to c . Without any calculation it may be understood, that the TR in $NdFeB$ is reduced in comparison with $SmCo_5$. One reason is the smaller switching field distribution, which reduces the asymmetry in the dc-demagnetized initial state. Furthermore, the nonmagnetic layer increases the distance between the magnetic grains and therefore reduces the divergence of the magnetization, what results in smaller field fluctuations. If one does not ascribe the observed TR in Sm_2Co_{17} to imperfections, one has to take into account the cell structure yielding the volume pinning mechanism. If a grain of such a magnet is switched, the domain wall moves by successively switching these cells, i.e. as switching units one has to regard now the cells, not the grains. Thus, also "single crystals" of Sm_2Co_{17} should ex-

hibit TR. This was indeed observed [20]. If the precipitation structure is perfect, all the cells will exhibit the same switching field, resulting in a very small switching field distribution, what reduces the TR considerably. The switching of adjacent cells will be very correlated, resulting in a movement of the domain wall. Furthermore the exchange coupling of neighboring cells will surely dominate over the dipole-dipole interaction due to the smallness of the cells. Although this may be partly taken into account by allowing for internal demagnetization factors n bigger than one, the averaging over the neighboring grains as was done by the inclusion approximation becomes very questionable. Thus, the presented theory may be not very suited for the case of Sm_2Co_{17} .

Regarding the data fitting we learned from Fig. 22 that both weak grains and down-switching of hard grains for higher temperatures has to be taken into account. This increased the computational effort considerably, due to the self-consistency requirements for $\bar{H}_s(T)$ and $\langle M \rangle$. The model parameters determined from the fitting procedure have to be considered as estimates. To increase their reliability improvements of both the theory, as outlined above, and the experimental data are necessary. Regarding the experiment, both labor experience and the presented theory show that the most critical point in a TR experiment is the sample demagnetization factor. Of course, a closed circuit measurement would be highly desirable, as was shown in the very first reported TR experiment. This is hard to realize, especially for high-coercive samples and at low temperatures. Therefore rotational ellipsoidal samples with the symmetry axis along the texture axis should be used to secure the homogeneity of the mean internal field. A second point is a very accurate measurement of $H_C(T)$ and $M_S(T)$. Especially the coercivity should be measured before and after a TR experiment, where measurements beyond T_{max} should be the last measurements at all, since they may result in irreversible changes within the material. Furthermore the field depen-

dence of the irreversible susceptibility should be determined for several temperatures, since this would allow to determine an estimate of the SFD and to proof the assumption that the temperature dependence of the switching fields of different grains are equal. Since the theory was extended to arbitrary starting points, small deviations from the dc-demagnetized state are no problem. On the contrary, different small steady fields should be applied during the TR experiment to determine the suppression field H' , as an experimental estimate of the field fluctuation width.

For the theory of the TR and ITR it was inevitable to develop a theory for the hysteresis and the recoil curves also. Whereas there exist a multitude of micro-magnetic calculations trying to explain the coercivity by assuming special micro-structures which give rise to either pinning of domain walls or nucleation, our theory starts a little above this level, since we do not judge about the reason for a switching field, but simply accept its existence. In this point the theory resembles the Preisach [36] model (PM). A theory of the TR based on the classical model is not able to explain TR effects of more than 50%. Furthermore this model was shown to have the congruency and wiping-out property [37], which is a severe disadvantage, since in most of the interesting cases the measured magnetization behavior violates these conditions. The main disadvantage of the classical Preisach model is due to the fact that the Preisach distribution function is not dependent on the magnetization state [36, 38]. To describe TR effects up to 100% it was necessary to take into account many-particle effects, i.e. the feedback of the neighborhood onto the grain, which result in a dependence of the form of the fluctuation field distribution on the magnetization state [10]. As shown above the TR model was further completed step by step by taking into account the contribution of multi-domain particles and by the inclusion approximation. Parallel in time and mainly in the context of recording media the classical PM was improved

also by taking into account a mean field shift [39, 40] in the moving PM (MPM). Although at first glance the "moving term" $H + k\langle M \rangle$ looks very similar, it describes a rigid mean field shift which is the same for all magnetic units. Contrary, the "inclusion correction" $H - n(\sigma M_S - \langle M \rangle)$ describes the deviation of the grain magnetization from the magnetization of its neighborhood. To take reversible processes into account the MPM was modified another time by allowing non-rectangular elementary hysteresis loops [41] of the magnetic units, or by splitting the Preisach density function, as it was done in [42, 43] (GPM). The common drawback of all the mentioned Preisach models is the neglect of the state and history dependence of the *form* of the interacting field distribution. This had been shown already by one of the first computer simulations [44], and also by experiments [45]. The variable variance Preisach model accounts partly for that observation [46]. If the improvements of the various mentioned Preisach models would be mounted together, it may be probably possible to describe the TR in permanent magnets also on that basis, if reasonable assumptions regarding the temperature dependence of the model parameters are added. A first step in this direction was done in Ref. [47].

In conclusion it can be said that the investigation of the TR and ITR may be used to characterize modern permanent magnet materials. In connection with the presented model it provides an alternative tool for studying interaction effects in relation to the temperature dependence of the saturation magnetization and switching field distribution.

References

- [1] B.G. Lifshits, A.S. Lileev, and V.P. Menushenkov, *Izv. Vuz. Chern. Metallurg.* **11** (1974) 140
- [2] from [1], translated from Russian by one of the authors (R. S.).
- [3] L.A. Kavalerova, B.G. Lifshits, A.S. Lileev, and V.P. Menushenkov, *IEEE Trans.*, **MAG 11** (1975) 1673
- [4] J.D. Livingston and D.L. Martin, *IEEE Trans.*, **MAG 20** (1984) 140
- [5] J.D. Livingston and D.L. Martin, *J. Appl. Phys.* **57** (1985) 4137
- [6] L. Jahn and R. Schumann, *phys. stat. sol. (a)* **91** (1985) 603
- [7] Lileev and Steiner, *Phys. Stat. Sol. (a)* **40** (1977) 125
- [8] B.G. Lifshits, A.S. Lileev, T.V. Abalyan and V.P. Menushenkov, *Izv. Vuz. Chern. Metallurg.* **11** (1976) 131
- [9] A.A. Zaytzev and A.S. Lileev, *Izv. Vuz. Chern. Metallurg.* **3** (1988) 74
- [10] R. Schumann and L. Jahn, *Proc. 6th Int. Seminar on Magnetism, Wiss. Zeitschr. HfV Dresden, Sonderheft 31* (1987) 65
- [11] K.-H. Müller, D. Eckert, and R. Grössinger, *J. de Physique* **49** (1988) C8 645
- [12] V.E. Ivanov, L. Jahn, *Fiz. Metall. i. Metalloved.* **75** (1993) 28
- [13] R. Scholl, L. Jahn, and R. Schumann, *phys. stat. sol. (a)* **102** (1987) K37
- [14] K.H.J. Buschow, A. S. van der Groot, *J. Less. Common. Met.* **14** (1968) 323
- [15] K.H.J. Buschow, F.J.A. Den Broeder, *J. Less. Common. Met.* **33** (1973) 191
- [16] L. Jahn, R. Schumann, and V. Ivanov, *IEEE Trans. Magn.* **37** (2001) 2506
- [17] A.S. Lileev, V.P. Menushenkov, and A.M. Gabay, *J. Magn. Magn. Mater.* **117** (1992) 270
- [18] Sample due to courtesy of W. Rodewald, Vacuumschmelze Hanau

- [19] H. Kronmüller, in "Supermagnets, Hard Magnetic Materials", p. 461, eds. G.J. Long and F. Grandjean, Kluwer Academic Publishers, Dordrecht, Boston, London, 1991
- [20] W. Ivanov, L. Jahn, phys. stat. sol. (a) **127** (1991)k117
- [21] L. Jahn, V. Ivanov, R. Schumann, M. Loewenhaupt, J. Magn. Magn. Mater **256** (2003) 41
- [22] L. Jahn, R. Schumann, J. Magn. Magn. Mater **251** (2002) 93
- [23] R. Schumann and L. Jahn, J. Magn. Magn. Mater. **232** (2001) 231
- [24] L. Jahn, H. Nagel, Wiss. Zeitschr. HfV Dresden **37**(1990)147
- [25] R. Schumann, P. Seidel, and L. Jahn, The Physics of Metals and Metallography 91, Suppl. 1 (2001) 257
- [26] P. Seidel, Diplomarbeit, TU Dresden, 2000
- [27] E.C. Stoner and E.P. Wohlfarth, Philos. Trans. R. Soc. **A240** (1948) 599
- [28] A.M. Gabay, A.S. Lileev, S.A. Melnikov, and V.P. Menushenkov, J. Magn. Magn. Mater **97**(1991) 256
- [29] R. Schumann and L. Jahn, The Physics of Metals and Metallography 91, Suppl. 1 (2001) 253
- [30] R.W. Chantrell, M. Fearon and E.P. Wohlfahrt, phys. stat. sol. (a) **97**(1986)213
- [31] K.H. Mueller, Proc. 6th Int. Seminar on Magnetism, Wiss. Zeitschr. HfV Dresden, Sonderheft 31 (1987)57
- [32] Yu.G. Pastushenkov, A.V. Shipov, R.M. Grechishkin, L.E. Afanasieva, J. Magn. Magn. Mater. **140-144** (1995) 1103.
- [33] A.A. Zaytzev and A.S. Lileev, Izv. Vuz. Chern. Metallurg. **11** (1989) 89
- [34] S. Hirosawa, K. Tokura, Y. Matsuura, H. Yamamoto, S. Fujimura and M. Sagawa, J. Magn. Mag. Mat. **61**, 363 (1986)
- [35] H. Kronmueller, K.-D. Durst, and M. Sagawa, J. Magn. Mag. Mat. **74**, 291 (1988)
- [36] F. Preisach, Z. Phys. **94** (1935) 277
- [37] I. M. Mayergoyz, Phys. Rev. Lett. **56** (1985) 1518
- [38] For a survey over Preisach models: E. Della Torre, *Magnetic Hysteresis*, IEEE Press, New York, 1999
- [39] E. Della Torre, IEEE Trans. Audio Electroacoust. **14** (1966) 86
- [40] V. Basso and G. Bertotti, IEEE Trans. Magn. **30** (1994) 64
- [41] E. Della Torre and F. Vajda, IEEE Trans. Magn. **30** (1994) 4987
- [42] T. Song, R. M. Roshko, E. Dan Dahlberg, J. Appl. Phys. **87** (2000) 4786
- [43] A. Stancu, P.R. Bissell, R. W. Chantrell, J. Appl. Phys. **87** (2000) 8645
- [44] R. Moskowitz and E. Della Torre, J. Appl. Phys. **38** (1967) 1007
- [45] M. Pardavi-Horvath and G. Vergesy, IEEE Trans. Magn. **30** (1994) 124
- [46] F. Vajda, E. Della Torre, M. Pardavi-Horvath, and G. Vertesy, IEEE Trans. Magn. **29** (1993) 3793
- [47] K.H. Müller, M. Wolf, D. Eckert and U.K. Rösler, Proc. 11th Int. Symp. on Magnetic Anisotropy and Coercivity in Rare-Earth Transition Metal Alloys, eds. H. Kaneko, M. Homma, M. Okada, The Japan Inst. on Metals, 2000